Florian Gobec, BSc

Towards clickable Metal Organic Frameworks (MOFs)

Synthesis of tetrazine based linkers

MASTERARBEIT

zur Erlangung des akademischen Grades

Diplom-Ingenieur

Masterstudium Technische Chemie

eingereicht an der

Technischen Universität Graz

Betreuer

Assoc. Prof. DI Dr. Christian Slugovc

Institut für Chemische Technologie von Materialien

Graz, August 2018

EIDESSTATTLICHE ERKLÄRUNG

Ich erkläre an Eides statt, dass ich die vorliegende Arbeit selbstständig verfasst, andere als die angegebenen Quellen/Hilfsmittel nicht benutzt, und die den benutzten Quellen wörtlich und inhaltlich entnommenen Stellen als solche kenntlich gemacht habe. Das in TUGRAZonline hochgeladene Textdokument ist mit der vorliegenden Masterarbeit identisch.

Datum

Unterschrift

Acknowledgement

I want to thank Prof. Slugovc for enabling me to work on this challenging topic and his support throughout the duration of my master thesis.

Furthermore, I want to thank my working group for providing a pleasant atmosphere during these last 6 months. Especially DI Petra Hofstadler was a great help for me during the duration of my thesis. She was always very helpful in every aspect where I needed support whether that was finding a chemical in the lab, organizing my masters exam, improving the layout of my master thesis and many other things. Additionally, I want to acknowledge the help of Dr. Petra Kaschnitz with her expertise on NMR-spectroscopy, Josefine Hobisch for the TGA-measurements, Dr. Ana Torvisco for the crystal structure analysis and Birgit Ehmann for providing all the needed chemicals.

As well I want to thank my family and friends for their never-ending support for me. Especially my parents who enabled this study and helped me along my whole life journey to the point where I am right now. Therefore, I want to thank them for making everything possible and always being there for me whenever I needed them. I also want to thank my girlfriend Yvonne for always standing by my side no matter the moods I had during my studies. Thanks for always being there for me, supporting me and bringing me back on track whenever I was confronted with tough situations. Additionally, I want to thank my best friend Daniel Dajakaj who although living in Vienna was always able to clear my mind and support me throughout my studies. Also, I want to thank Lukas Ladenstein who supported me throughout my studies as a study colleague as well as a friend who I could always count upon.

Abstract

Metal organic frameworks (MOFs) have experienced some extraordinary advances in research due to their great variety of potential structures and applications. Due to these circumstances and their great potential, they have established themselves as an interesting field of study. They consist of the linkage of metal ions or clusters through coordinative bridges of linkers. These linkers have a great influence into the overall topology and the properties of the formed frameworks. Therefore, this thesis focuses on the synthesis of various potential organic linkers for their application in different MOFs containing either Zn^{2+} or Fe^{3+} as metal ions. They were based on different N-heterocyclic compounds that were at first alkylated with either methyl or tert-butyl acrylate via a so called aza-Michael addition reaction. Subsequently they were saponified under acidic conditions and further reacted with different metal salts to MOFs. For characterization NMR, IR, single crystal XRD and TGA measurements were performed. Additionally, a potential tetrazine-based organic linker was synthesized starting with imidazole-2-carbonitrile. For the improvement of the synthesis of this linker also different catalysts (metal catalyst and sulfur) were tried. For the characterization of this compound NMR-measurements were performed.

Kurzfassung

Metallorganische Gerüstverbindungen (**m**etal **o**rganic **f**rameworks, MOFs) haben aufgrund ihrer großen Vielzahl an potentiellen Strukturen und Anwendungen das Interesse vieler Forscher geweckt. Aufgrund ihres großen Potentials haben sich MOFs als eigenständiges Studiengebiet etabliert. Diese Verbindungen bestehen aus Metallionen oder Metallclustern die durch koordinative Bindungen von Liganden, den so genannten Linkern, miteinander verbunden werden. Diese Linker haben einen großen Einfluss sowohl auf die Topologie als auch auf die Eigenschaften der daraus entstehenden Gerüstverbindungen. Deshalb liegt der Schwerpunkt dieser Arbeit auf der Synthese von verschiedenen potentiellen organischen Linkern und deren Einbindung in verschiedene Gerüstverbindungen basierend auf Zn^{2+} und Fe^{3+} Metallionen. Die besagten Linker basierten auf N-heterozyklischen Verbindungen die mit methyl oder tert-butyl Acrylaten via einer so genannten aza-Michael Addition alkyliert wurden. Anschließend wurden die Estergruppen unter sauren Bedingungen hydrolysiert und mit verschiedenen Metallsalzen zu metallischen Gerüstverbindungen umgesetzt. Für deren Charakterisierung wurden NMR, IR, Einkristall XRD und TGA Messungen durchgeführt. Des Weiteren wurde ein potentieller, auf einem Tetrazin basierender, organischer Linker ausgehend von Imidazol-2-carbonitril synthetisiert. Um diese Synthese zu optimieren wurden verschiedene Katalysatoren (Metallkatalysator und Schwefel) getestet. Zur Charakterisierung dieser Verbindung wurden NMR-Messungen durchgeführt.

List of Abbreviations

BET	Brunauer-Emmet-Teller
Bzm	benzimidazole
DCM	dichloromethane
dhtz	dihydrotetrazine
dipydz	3,6-bis(4-pyridyl)-1,2-diazine
dipytz	di-3,6-(4-pyridyl)-1,2,4,5-tetrazine
DPT	3,6-di(pyridin-4-yl)-1,2,4,5-tetrazine
EDG	electron donating group
EtOAc	ethyl acetate
EtOH	ethanol
EWG	electron withdrawing group
Im	imidazole
IR	infrared
IRMOF	isoreticular MOF
MeOH	methanol
MIL	matériaux de l'institut lavoisier
mIm	methylimidazole
MOF	metal organic framework
PCP	porous coordinated polymer
PhIm	phenylimidazole
PSM	post synthetic modification
Pyr	pyrazole
SBU	secondary building unit
SCO	spin crossover
STA	St. Andrews university
TGA	thermogravimetric analysis
Tri	triazole
tz	tetrazine
UiO	Universitetet i Oslo
ZIF	zeolitic imidazolate framework

Table of Content

1 Introduction

MOFs or Porous coordination polymers (PCPs) are a compound family which has a polymeric framework with regular tunable pores.[1–5] Compounds like these are known since the early 1960s[6] and have since then been readily researched upon. What makes this compound family so fascinating is that they show a high designability, structural diversity, flexibility and regularity. Regularity means that the framework shows a regular pore distribution, which is important for adsorption. The regularity is achieved due to the crystalline form of the MOF.[7] Due to these versatile and tunable properties there are a lot of possible applications in which MOFs are used such as gas purification[8], storage for energy gases like methane, carbon dioxide, hydrogen or water[9–13], treatment for nuclear waste water[14], for catalysis[15–19] and even as a potential multi carrier of drugs.[20] For the synthesis of PCPs at least a metal ion and a so called linker is needed. For metal ions different metals can be used to form MOFs. In the beginning of the research into these compounds the main focus was on transition metals like Cu(I, II), Ag(I), Zn(II), Cd(II) and Co(II) but due to their relative high costs and for some cases low abundances the overall costs for MOFs were quite high. That is why metal ions with lower costs and higher abundances were researched for the formation of said frameworks like Al(III), Mg(II), Ca(II), Fe(II), Na(I) and K(I).[7] As a linker, also known as spacer, between said metal ions, different inorganic and organic molecules are used.[1] For inorganic ligands halides or cyanides are used due to their bridging abilities.[21–23] For used organic ligands it can be differentiated between neutral, such as N-based linkers like imidazole, pyridine or bipyridine, anionic like carboxylate based linkers and cationic ligands.[24–27] Said linkers have a great influence in the overall topology of the formed MOFs as their shape, size and mutual angle between them effect network topologies and properties of the frameworks.[28,29] If a functionalized organic linker is implemented in the framework the possibility of a so called postsynthetic modification (PSM) exists. A PSM is defined as a chemical alteration to the MOF-lattice after it has been synthesized.[30] These kinds of modifications are used to fine-tune chemical and physical properties of MOFs.[31,32] PSM is a great feature to control the type as well as also the number of functional groups that get incorporated in the framework. With this approach it is possible to synthesize topologically identical frameworks with differing functionality.

Furthermore, it is possible to functionalize the metal and the organic parts of the framework while the stability of the MOF is not affected.[30,32,33] Some prominent MOFs are e.g. MOF-5, also called IRMOF-1, ZIF-8 or MIL-53(Fe). Their solid-state structures are depicted in Figure 1 below.

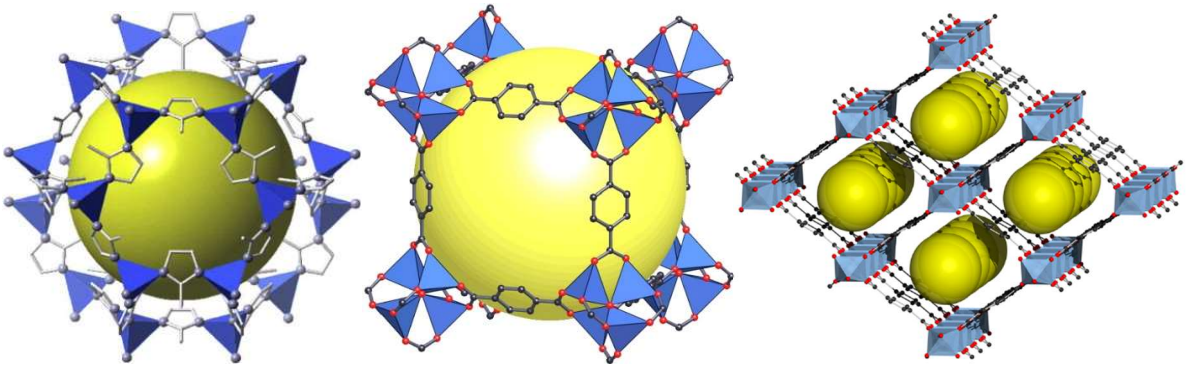

Figure 1: *from left to right: ZIF-8[34], MOF-5[35] and MIL-53[36]; the yellow ball indicates the free space in the frameworks*

Zeolitic imidazolate frameworks (ZIF) are a subclass of MOFs and consist of a metal ion, mostly Zn(II) or Cd(II), and an imidazolate linker.[37] MOF-5 consists also of Zn(II) as a metal ion but uses a dicarboxylate ligand, namely terephthalic acid, as a linker.[38] MIL-53 is a MOF which has Al(III) as a metal ion and also terephthalic acid as a linker.[39] There also exist structure analogues with different trivalent metals like Fe and Cr.[40,41] A MIL in which the metal ion was changed from Al(III) to Fe(III) is then denounced as MIL-53(Fe).

The focus of this master thesis is the synthesis of a novel tetrazine based organic linker for the application in MOFs. Therefore, different pre-assessment experiments regarding the precursors, several substituted aromatic N-heterocyclic compounds, had to be made. Also, the change in characteristics regarding different alkylation reactions and different saponification conditions on these compounds shall be investigated. Additionally, to gain further insight in the formation behavior of MOFs, different metal ions will be used and compared regarding their properties and formed products. For the tetrazine based linker different catalytic options will be investigated and differences between symmetrically and asymmetrically substituted tetrazines shall be researched and compared.

2 General Aspects

2.1 Metal organic frameworks (MOFs)

2.1.1 Carboxylate based MOFs

A representative for this class is the previously mentioned MOF-5. This class of MOFs consists of a metal ion and a dicarboxylate ligand. The used carboxylate-based bridging ligands used in these frameworks are of particular interest because on the one hand the underlying carboxylic acid can be deprotonated for charge balance and on the other hand it can bind metals in various ways.[42] Due to these circumstances the possibility to achieve multidenticity with these types of ligands is possible which makes them even more interesting to use. With the implementation of the carboxylate-based ligand, to be more specific, multidentate carboxylate ligands, quite rigid frameworks can be formed. This is because of their ability to aggregate the present metal ions into M-O-C clusters, which are so called secondary building units (SBUs). Out of these SBUs it is now possible, due to the beforehand mentioned multidenticity of some carboxylate-based ligands, to polymerize them into an extended network, the MOF. The rigidity of the framework is now established because the metal ions are held in their positions by the carboxylate groups. The SBUs are now serving as vertices which can be joined by rigid organic links to form a MOF. As additional feature the formed frameworks are neutral which makes the implementation of counterions in the cavities obsolete.[43] A representation of such a formation of an MOF is depicted in Figure 2.

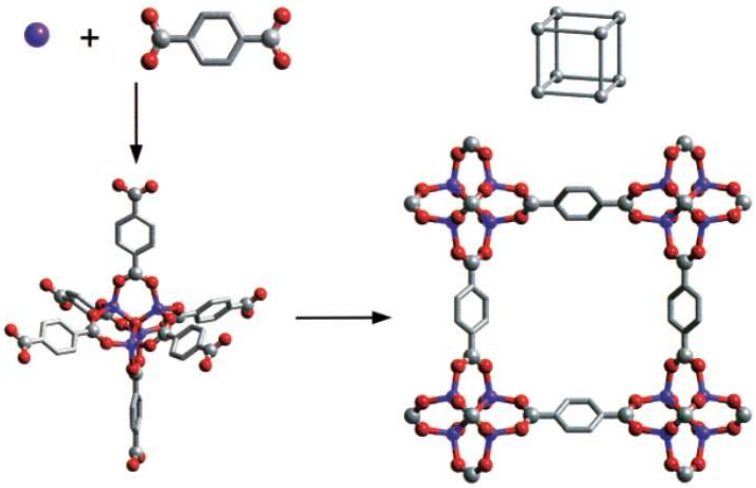

Figure 2: *formation of a MOF out of a metal (violet) and terephtalic acid; O (red), C (grey)*[43]

The formed SBUs now impact the overall pore size and porosity of the whole framework. Depending on the size of the used carboxylate bridging ligand there can be achieved different pore sizes. A visual representation of this fact is presented in Figure 3 where Eddaoudi et al. synthesized based on the structure of MOF-5 using different carboxylate ligands various frameworks which also differ in their pore sizes.

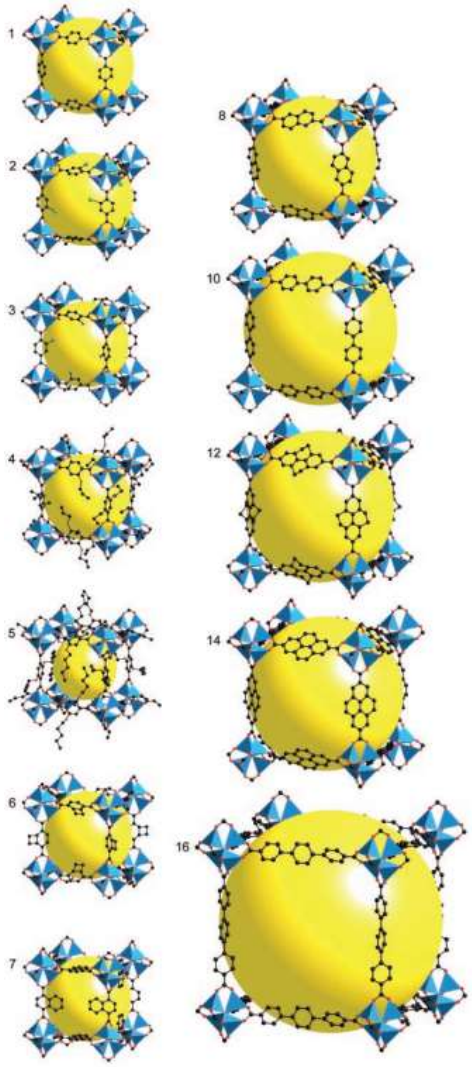

Figure 3: *comparison of the effect of using different carboxylate bridging ligands on the pore sizes of MOFs*[44] *the yellow ball indicates the free space in the frameworks*

Another feature of these carboxylate-based frameworks is their high surface area. The BET surface area of the prominent MOF-5 is 3800 m^2/g. This can be even more improved when using different carboxylate-based ligands. So, similar frameworks like MOF-200 and MOF-177 with respectively different used ligands have BET surface areas of 4746 and 6260 m^2/g.[45,46] The usual synthetic approach to such carboxylate-based MOFs are solvothermal methods but recently also microwave syntheses have been applied.[9,47]

2.1.2 Iron containing MOFs

As the name already suggests these frameworks have iron as their metal ion and differ additionally in their used ligands. They were initially researched as an alternative to Zn(II) and Cu(II) based MOFs because due to their quite weak bond to their ligands the formed frameworks show poor chemical stabilities and are prone to hydrolysis. A potential solution for this problem was the research into trivalent metal ions like Fe(III), Cr(III) or V(III) for their usage in MOFs. This may now solve before mentioned problem but creates a new one as the controllability for the formation of a MOF gets more difficult because of the higher reactivity of said metal ions.[48] Another reason why Fe(II or III) based MOFs are an interesting field of study is as mentioned in chapter 1 the relative low cost and high abundance of these metals.

An overview of some of the used ligands for either bivalent or trivalent iron ions in MOFs shall be presented in the following paragraphs.

Wharmby et al. use a phosphonate-based ligand with a bivalent iron to form a framework called STA-12(Fe) which possesses a BET surface area greater than 1000 m^2/g and pore sizes of approx. 10 Å.[49,50]

There are also similar structures as described in chapter 2.1.1 where iron is used as a metal ion and carboxylate-based ligands as linkers. An example for such a MOF is the before mentioned MIL-53(Fe). A big advantage of this framework is the ability to functionalize it by using carboxylate-based ligands with polar/apolar or acidic/basic groups.[51] Another interesting feature of this framework is that it can occur in three different forms. Form one is called as synthesized (as) and has still some unreacted ligand within the tunnels. The second one is called open and only occurs at high temperatures. When cooling the second form down a water molecule is trapped within the tunnels, which leads to a radical shrinkage of the MOF of approx. 40%. This resulted third form is called hydrated due to the entrapped water molecules.[52]

2.1.3 Zeolitic imidazolate frameworks (ZIFs)

As already mentioned in chapter 2 a ZIF is a subclass of metal organic frameworks. They consist of different metal ions and imidazolate linkers. The SBUs contain M-Im-M with Zn or Co as M and different imidazolate linkers as Im.[53] The formed structures of these ZIFs are similar to those of inorganic aluminosilicate zeolites.[54] The Zn(II) takes the role of the silicone and the imidazolates, due to their anionic character, form ligand-bridges similar to the oxygens in zeolites as the angle between these bridging ligands is also approx. 145°(between N and N in 1,3-position of the ring).[55] With this additional feature ZIFs possess characteristics of MOFs as well as aluminosilicate zeolites. Furthermore, they are possible to combine the advantages of both of these compound families which makes them interesting to do research upon. ZIFs form an inorganic-organic network type with over 100 different topologies, thermal stabilities from up to 500 °C, high chemical stabilities in organic and aqueous media and a variety of chemical functionalities with organic linkers.[53,56] An overview of some of the different structures of ZIFs is presented in Figure 4.

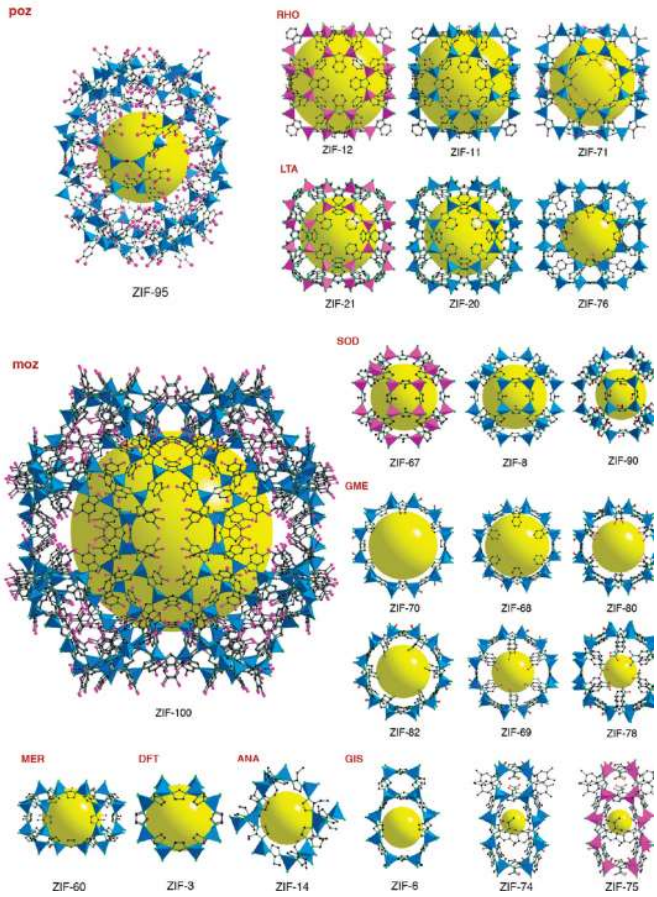

Figure 4: *overview of different existing ZIFs grouped according to their topology (three letters above structures) with ZnN_4 as blue and, CoN_4 as pink polyhedral, C in black, N in green , O in red and Cl in green; the yellow ball indicates the free space in the frameworks*[56]

The net topologies of these ZIFs are directed through imidazolate link-link interactions combined with the composition of the solvent used for the synthesis. Therefore, it is possible to tune the structure and topology of ZIFs by varying the used imidazolate-based ligands.[57,58]

Furthermore, it is possible to use PSM to functionalize ZIFs while keeping their overall structure intact. This was proven by Morris et al. by reducing or reacting ZIF-90 with different reagents to obtain ZIF-91 and ZIF-92. With $NaBH_4$ it is possible to reduce ZIF-90 to form ZIF-91 and when reacted with ethanolamine ZIF-92 is obtained[59]. A simplified scheme of this fact is depicted in Scheme 1 below.

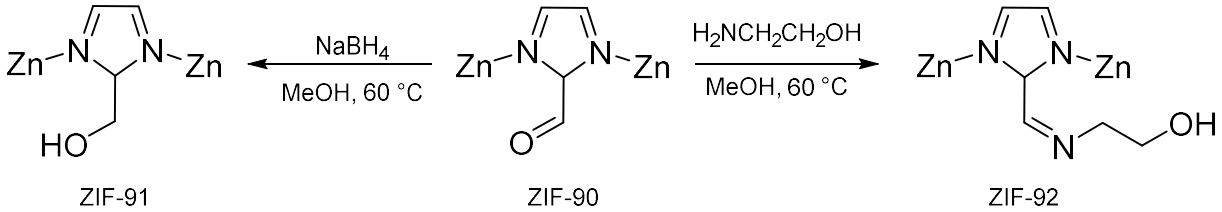

ZIF-91 ZIF-90 ZIF-92

Scheme 1: *PSM of ZIF-90 to form ZIF-91 and ZIF-92*

2.2 (New) imidazole-based linkers

As already mentioned in chapter 2.1.3 the used linker for these frameworks, imidazolates, plays an important role in the topology and the formation of the framework itself. This chapter will focus on said linkers and their influence on the formed frameworks and the take on new imidazole-based linkers.

In general imidazole is an N-heterocyclic compound consisting of a five-membered ring with two N-donor coordination sites. There is also the possibility to derivatize this compound at positions 1,2 or 4 of the ring.[60] This makes the compound so interesting because it can now implement functional groups into the framework making them versatile compounds with various new properties.[61,62] Additionally to imidazole there are also other N-heterocyclic compounds that are of interest for the use as organic linkers for MOFs like triazoles, tetrazoles and pyrazoles.[63,64] The imidazole itself can now be used as a donor for Lewis acidic metal ions, acting as a neutral monodentate ligand or deprotonated, forming an imidazolate anion, and be used as an anionic bidentate bridging ligand.[60,65] Additionally, for the use of carboxylate-based and imidazole derivates it is also possible to protonate the imidazole forming an acid-base co-crystal moiety.[66]

The used 1-imidazole containing ligands can now either function as rigid or as flexible ligands. Ditopic and tripodal imidazole-containing ligands are efficient building units for frameworks as they can react easily with various metal salts leading to numerous MOF-structures. These ligands are neutral, and the corresponding anions should already be incorporated into the MOF to balance the positive metal ion charges.[67–69] The introduced anions themselves have now also a strong impact on the overall structure of the MOF, as they can exist as terminal, dissociative or bridging ligands.[70] In contrast to rigid ligands, that show quite predictable structures, flexible ones show more variety regarding structures owing to their flexibility. This is possible as they are able to adopt to various confirmations according to the requirements of the used metal ions.[60]

Used 2-imidazole containing ligands on the other hand have two available N-donor atoms. This contrasts with the before mentioned 1-imidazole containing ligands where only one N-donor atom is available. This enables this kind of ligands to be anionic and bidentate, if deprotonated, additionally to being neutral and monodentate. Again, in addition to the used ligand in proto- or deprotonated form the used metal ions to form the MOF influence the overall structure of the framework.[60] Another feature of these ligands is that they are able to act as hydrogen bonding donors or acceptors which benefits the formation of MOFs.[71,72]

Combinations of carboxylate and 1-imidazole ligands have already shown to be effective in the formation of MOFs. A feature of this combination of ligands in a framework is that while the main ligand and the metal center are fixed the auxiliary linker is able to act structure directing during the formation of the framework.[73–75] For this thesis the combination effects on MOFs shall be further investigated. Especially how the alkylation of an imidazole-based ligand effects the formation of a MOF. By alkylating the imidazole-based ligand the negative charge gets further away from the ring. This also leads to a prolonged ligand which may have different impacts on the formation and the structure of the framework. A visualization of this theory is presented in Figure 5 below.

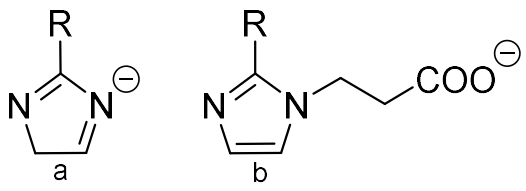

Figure 5: *illustration of unalkylated imidazolate (a) and alkylated mixed imidazolate carboxylate ligand (b)*

2.3 Tetrazine-based organic linkers in MOFs

Another interesting used organic linker for the formation of MOFs are tetrazine-based linkers. This chapter will give an overview as to why they are so attractive to investigate as such and how they are used in various MOFs.

Nickerl et al. implemented dihydro-1,2,4,5-tetrazine-3,6-dicarboxylate (dhtz) into the MOF UiO-66 by a postsynthetic linker exchange reaction. This way an optical sensor material for the detection of oxidative agents was developed. To be precise the dihydro-tetrazine linker was chosen to sense NO_x because it can be quite easily oxidized into the 1,2,4,5-tetrazine-3,6-dicarboxylate (tz). During this oxidation the linker system experiences a drastic color change as the dhtz is yellow and the tz pink. Another feature of this linker is that the reaction is reversible. Nickerl et al. used sodium dithionite as a regeneration agent to reduce the tz-MOF again to the dhtz-MOF. The successful back reaction could be observed by eye as the color changes back to yellow. The redox reaction including the visible change from yellow to pink of this MOF is presented in Figure 6 below.

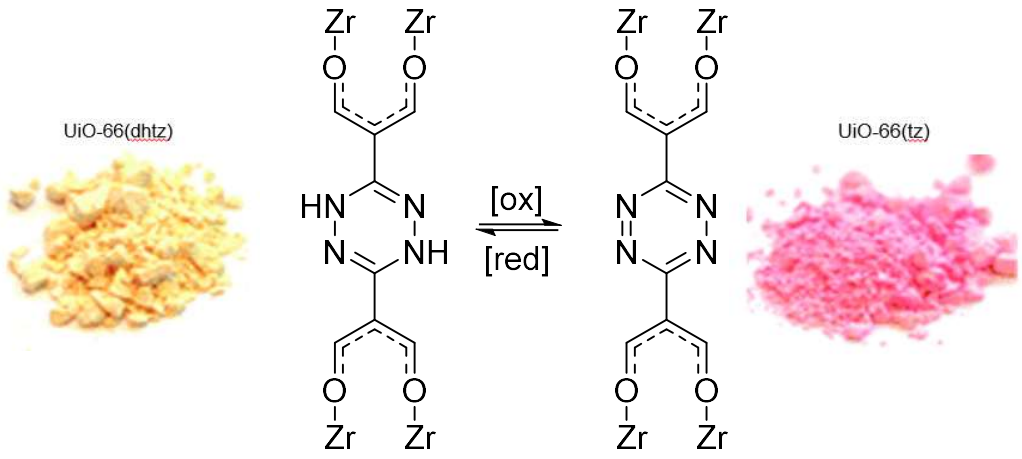

Figure 6: *redox reaction of UiO-66 with dhtz (yellow)/tz (pink)*

Additionally, to NO_x it was also possible to oxidize the dhtz-MOF with bromine in chloroform and with dihydrogen peroxide. But whereas the oxidations with NO_x and bromine showed immediate color changes the oxidation with dihydrogen peroxide took several minutes and the color change was gradually and not immediate.[76]

Razavi et al. also use a tetrazine based linker for their MOF for cation sensing. Therefore, they use 3,6-di(pyridin-4-yl)-1,2,4,5-tetrazine (DPT) in a combination with 4,4′-oxybis(benzoic acid) (H_2OBA) as spacers and Zn^{2+} as a metal ion to form MOF TMU-34(-2H) to sense cations, especially Hg^{2+}, by the photoluminescence method. They implemented DPT into their MOF because as mentioned before this kind of linker shows reversible redox activity with significant color changes. Additionally, DPT has low lying π^*-orbitals making it applicable for the use in sensors, electrochemistry and conductive materials. The four lone pairs of the nitrogen of the MOF can act as Lewis basic sites and as electron-donating motifs. Therefore, it is able to engage in hydrogen bonding with the hydrogens in water. Due to this hydrogen bonding electron density is shifted from the tz to the hydrogens of the water molecule, which equals reduced fluorescence emission intensity. They were able to detect Hg^{2+}selectively in acetonitrile as well as in water enabling them to simultaneously combine these two signal transductions which eliminates effects towards other cations and increases the sensitivity towards Hg^{2+}.[77]

Mouchaham et al. synthesized a MOF named MIL-163 using a tetrazine based linker. As tz-linker they used (1,2,4,5-tetrazine-3,6-diyl)bis(benzene-1,2,3-triol) (H_6-TzGal) combined with Zr^{4+} as metal ion. This MOF crystallizes in a tetragonal structure where TzGal chelates four Zr-ions. In the generated 3D open framework large square shaped interconnected channels could be observed. The thermal behavior of this framework was evaluated by TGA. It experiences in comparison to comparable Zr-MOFs a quite low decomposition temperature of approx. 210 °C. This could be due to the oxidative degradation of the linker material. Nonetheless this framework shows flexible behavior and great long-term chemical stability in aqueous media. This high chemical stability is due to a great strength of the metal-ligand bond, the solubility of the components and the presence of coordinatively accessible metal sites.[78]

Calaharro et al. synthesized a 3,3′- (1,2,4,5-tetrazine-3,6-diyl)dibenzoic spacer which they implemented into Zn- and La-MOFs. Said tz-based linker is a symmetrical multidentate bridging ligand where the two benzoic groups are used to bond with the metal ions and the tetrazine offers a π-acceptor function. A feature of the used tz is that due to its low-lying π^*-orbital it experiences strong π-accepting characteristics which in return lead to excellent electronic communication between the different metal ions throughout the framework.

Additionally, they reported the luminescence and adsorption properties of the designed MOFs and the in vitro cytotoxicity of cells of the linker. The result was that the cytotoxicity was negligible which opens up the potential application for the linker in MOFs in the biomedical field. The synthesized Zn-MOF shows a 2D structure whereas the La-MOF is a 3D structure with interesting channels.[79]

As already mentioned before due to the electron rich conjugated π-system of the tetrazine it can improve the interaction of a MOF with hydrogen. Chang et al. researched the synthesis, structures and hydrogen adsorption properties of a Zn-MOF with a tetrazine-based ligand. They used di-3,6-(4-pyridyl)-1,2,4,5-tetrazine (dipytz) as the ligand for their framework. For thermal properties a TGA measurement was performed which showed that said framework experiences decomposition at approx. 205 °C. For the pore characterization following values were determined: 402 m^2/g BET surface area and a micropore volume of 0.19 cm^3/g. Furthermore, the hydrogen adsorption was measured and showed that for this system the interaction between hydrogen and the framework is quite high.[80]

Clements et al. investigated the PSM of a dipytz containing Fe-MOF. This MOF is of a subclass which exhibits so called spin crossover (SCO). This is a phenomenon occurring in certain d^4 to d^7 transition metal complexes where high-spin (HS) and low-spin (LS) states can be accessed with the same material by external agitation. For the PSM the Inverse-electron-demand Diels-Alder (iEDDA) reaction with 2,5 norbornadiene was chosen. The result of this reaction is the formation of 3,6-bis(4-pyridyl)-1,2-diazine (dipydz). The reaction scheme is presented in Scheme 2.

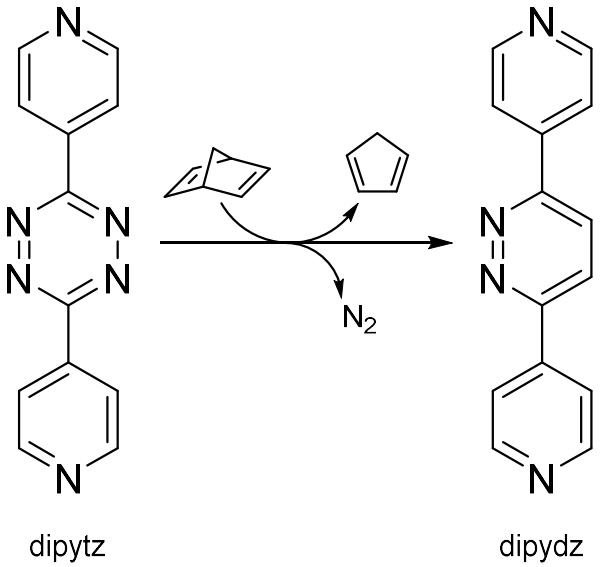

Scheme 2: *iEDDA reaction of dipytz with 2,5 norbornadiene to form dipydz*[81]

The PSM conversion of dipytz to dipydz was >95% and the process was observable via the naked eye due to a visible color change from purple, dipytz, to yellow, dipydz. They also showed that due to this conversion the more electron rich diazine is formed which increases the electron-donating ability of the ligand. Furthermore, there were small changes in the overall framework geometry observable, possibly due to the loss of two possible interframework hydrogen bonding sites.[81]

3 Results and Discussion

3.1 Aza-Michael Addition

For this master thesis several substituted aromatic N-heterocyclic compounds were prepared. An overview of the synthesized compounds is presented in Figure 7.

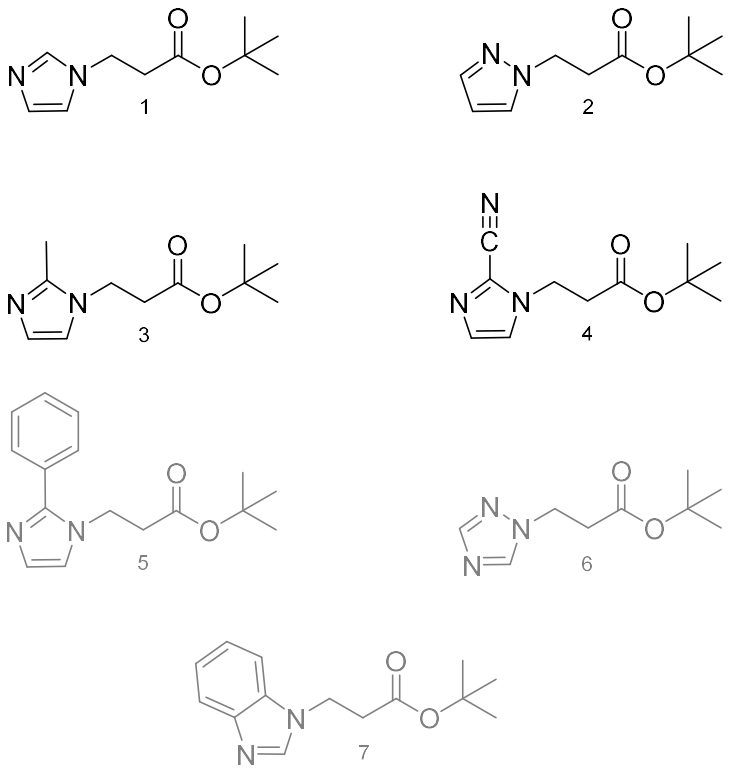

Figure 7: *prepared substituted N-heterocyclic compounds **1** to **7***

All these compounds were synthesized via the so-called Aza-Michael addition, a conjugate addition reaction. In general, these reactions need a solvent and catalyst to achieve acceptable yields and are usually not done in bulk.[82,83] For these reactions tert-butyl acrylate, an α,β-unsaturated compound, serves as the Michael acceptor whereas the N-heterocyclic compound as a Michael donor. The resulting products are so called β-amino carbonyl compounds. The big advantage of the synthesis of compounds **1** to **7** is, that they are done in bulk, without adding any solvent or catalyst. The general procedure for the synthesis of these compounds was the following. To the N-heterocyclic compounds, tert-butyl acrylate was added, and the mixture was put into the drying oven at 80 °C. When the heterocyclic compound was dissolved in the acrylate a ^{1}H-NMR measurement was performed, to check the reaction progress. When the reaction was complete the excess acrylate was removed via an N_2-stream over the solution.

A scheme of the general procedure of the synthesis is presented in Scheme 3.

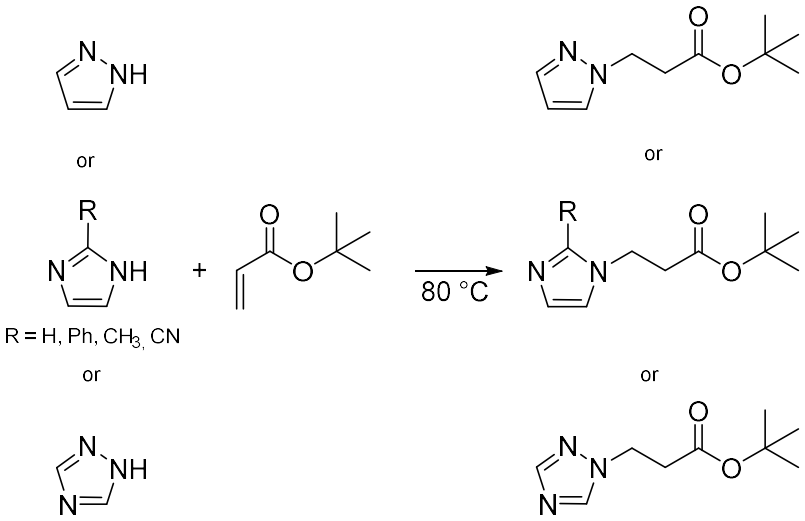

Scheme 3: *general synthesis of N-heterocyclic compounds*

The reaction is typically completed after 24 h. An overview of reaction time and the reaction yields of compounds **1** to **7** is presented in Table 1 below.

Table 1: *overview of reaction time and yield of the synthesis of compound **1** to **7***

compound	reaction time [h]	yield [%]
1	23	>99
2	25	73
3	20	93
4	20	90
5	23	81
6	23	36
7	23	92

The characterization of **1** to **7** was done via NMR measurements. Because of these results, additionally to the results presented in Table 1, the focus in the further investigations of the compounds narrowed down to compounds **1** to **4**. Further research into compounds **5** to **7** was neglected, due to either poor solubility of the N-heterocycle in the tert-butyl acrylate as in the case of the 1,2,4-triazole where the compound did not dissolve completely in the Michael acceptor and so no high yield of desired compound **6** was obtainable. In the other cases of compounds **5** and **7** where the conversion would have been acceptable, the NMR spectra revealed the presence of undesired side products of unknown identity.

In Figure 8 exemplary ^{1}H-NMR spectra of 1H-pyrazole and tert-butyl 3-(1H-pyrazol-1-yl)propanoate are depicted.

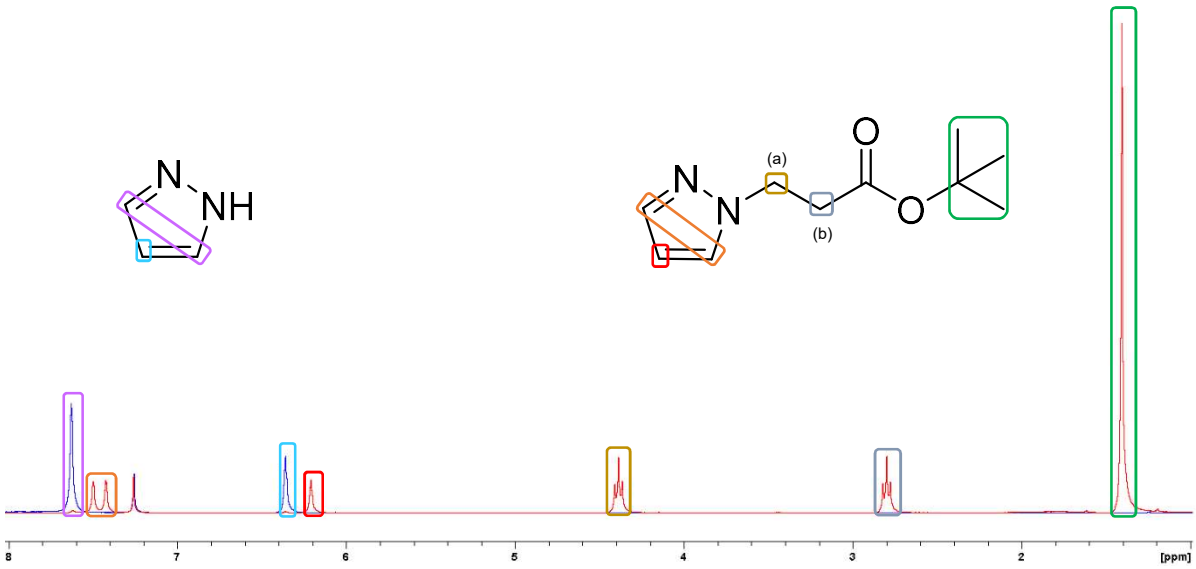

***Figure 8**: ^{1}H-NMR spectrum of tert-butyl 3-(1H-pyrazol-1-yl)propanoate(red) and 1H-pyrazole (blue) in $CDCl_3$*

For the alkylation of 1H-pyrazole and the other N-heterocycles to form their respective compounds **1** to **4** the formation of the triplets assigned to the ethylene bridge is characteristic. Additionally, the signals of the N-heterocycles show different shifts when alkylated and the characteristic signal for the tert-butyl group is observed. As seen in Figure 8 1H-pyrazole exhibits only two peaks. The two hydrogens of C^3 and C^5 show the same shift at 7.63 ppm and the hydrogen at C^4 correlates with the signal at 6.36 ppm. Also, the hydrogen of the C^4 experiences a shift to lower ppm. As already mentioned the characteristic of these ^{1}H-NMR spectra are the formation of the ethylene bridge of the different N-heterocycles. But the different compounds **1** to **4** show different shifts of the -CH_2. These different shifts of said ethylene groups of compounds **1** to **4** are summarized in Table 2.

Table 2:** summary of ^{1}H-NMR shifts of the two -CH_2 groups of compounds **1** to **4

compound	N-heterocycle	-CH_2 (a) [ppm]	-CH_2 (b) [ppm]
1	imidazole	4.22	2.70
2	pyrazole	4.39	2.80
3	2-methylimidazole	4.09	2.61
4	2-cyanoimidazole	4.40	2.77

In comparison with the shifts of tert-butyl 3-(1H-imidazol-1-yl)propanoate, **1**, the substitution of the C^2 of the imidazole compound with either an electron withdrawing group (EWG), as in the case of **4**, or electron donating group (EDG), as in the case of **3**, changes mentioned shifts of the $–CH_2$ groups (a) and (b). We can see that for tert-butyl 3-(2-methyl-1H-imidazol-1-yl)propanoate, **3**, where we have an electron donating methyl group that the shifts occur at lower ppm than with the unsubstituted **1**. Whereas for tert-butyl 3-(2-cyano-1H-imidazol-1-yl)propanoate **4**, which is substituted with an electron withdrawing cyano group, we can observe shifts at higher ppm than with the unsubstituted **1**.

In Table 3 the shifts of the ethylene groups in the ^{13}C-spectra of compounds **1** to **4** are summarized.

Table 3**: summary of ^{13}C-NMR shifts of the two -CH_2 groups of compounds **1** to **4

compound	N-heterocycle	-CH_2 (a) [ppm]	-CH_2 (b) [ppm]
1	imidazole	42.75	37.30
2	pyrazole	42.82	36.38
3	2-methylimidazole	41.69	36.79
4	2-cyanoimidazole	43.23	36.44

As already seen in the case of the shifts in ^1H-NMR spectra we can now observe a similar trend in the ^{13}C-spectra. The signals for both ethylene groups of **3** with the EDG are shifted again to lower ppm in comparison to the unsubstituted **1**. For the EWG containing compound **4** both ethylene groups experience different shifts. Ethylene group (a) gets again shifted to higher ppm, whereas group (b) is shifted to lower ppm in comparison with compound **1**.

3.2 Saponification reactions of N-heterocyclic compounds

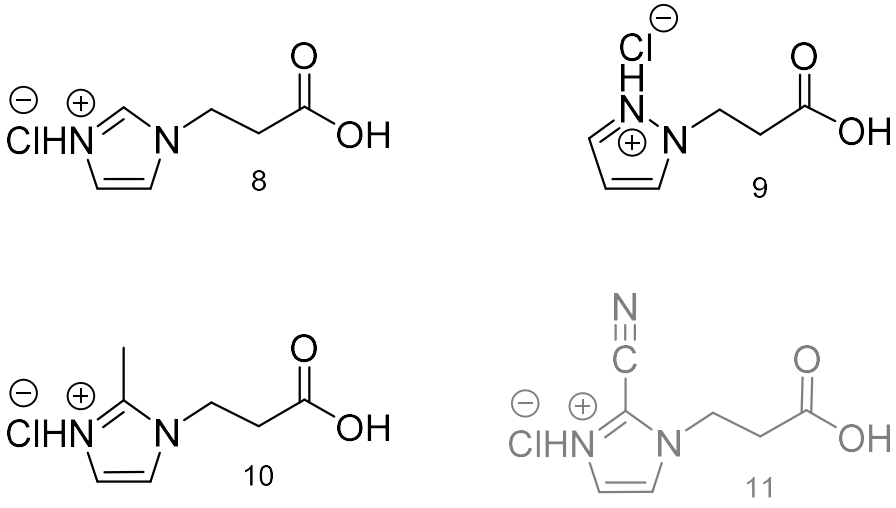

Figure 9: *overview of the prepared saponified N-heterocyclic compounds*

For the use as linkers in MOFs, the next synthetic step is the saponification reaction of the N-heterocyclic compounds **1** to **4**. Therefore 1 eq of said compound was reacted with 2 eq of aqueous HCl and stirred at 80 °C in an open vial while scrubbing the water. This was done until solidification occurred and no stirring was possible anymore. The reaction progress was then checked via NMR measurements in D_2O. Said progress is easily traceable via the observable disappearance of the peak of the tert-butyl group. Further research into compound **11** was neglected at this point as the focus with the precursor of this compound was the synthesis of a tetrazine based organic linker for MOFs as mentioned in chapter 3.4.3. An overview of the synthesized compounds and their proposed structure is presented in Figure 9.

Additionally, to the proposed protonated structures there is also the possibility that the compounds occur in their deprotonated state. To determine which case is more probable ^{1}H, ^{13}C-NMR and IR measurements were performed. The determination of the most probable structure was done exemplary for all presented compounds with 1-(2-carboxyethyl)-1H-imidazol-3-ium chloride, **8**. Furthermore ^{1}H-, ^{13}C-NMR and IR spectra of sodium 3-(1H-imidazol-1-yl)propanoate, synthesized by Katharina Kodolitsch, was used to determine the most likely structure of compounds **8** to **11**. In Figure 10 depicted below a comparison of sodium 3-(1H-imidazol-1-yl)propanoate and **8** is presented.

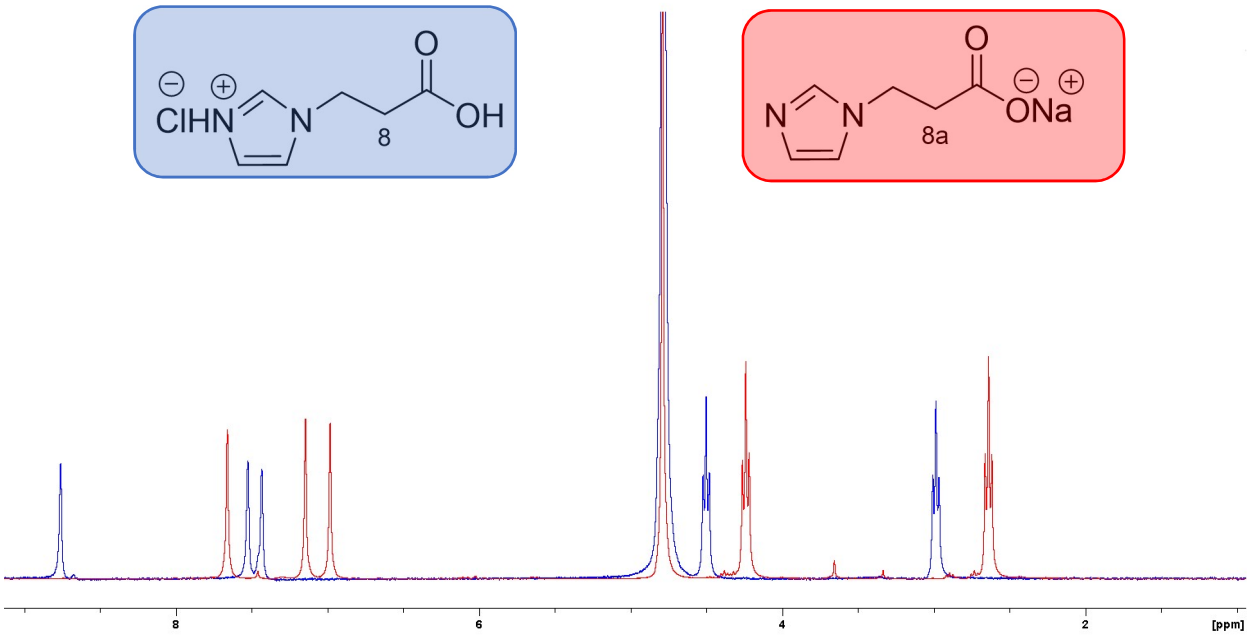

Figure 10: *comparison of ^{1}H-NMR spectra of sodium 3-(1H-imidazol-1-yl)propanoate (red) and* ***8*** *(blue) in D_2O*

It can be seen that all the peaks of the protonated compound **8** are shifted to lower field in comparison to the deprotonated sodium 3-(1H-imidazol-1-yl)propanoate **8a**. The comparison of the IR-spectra of these two compounds **8** and **8a** is presented in Figure 11.

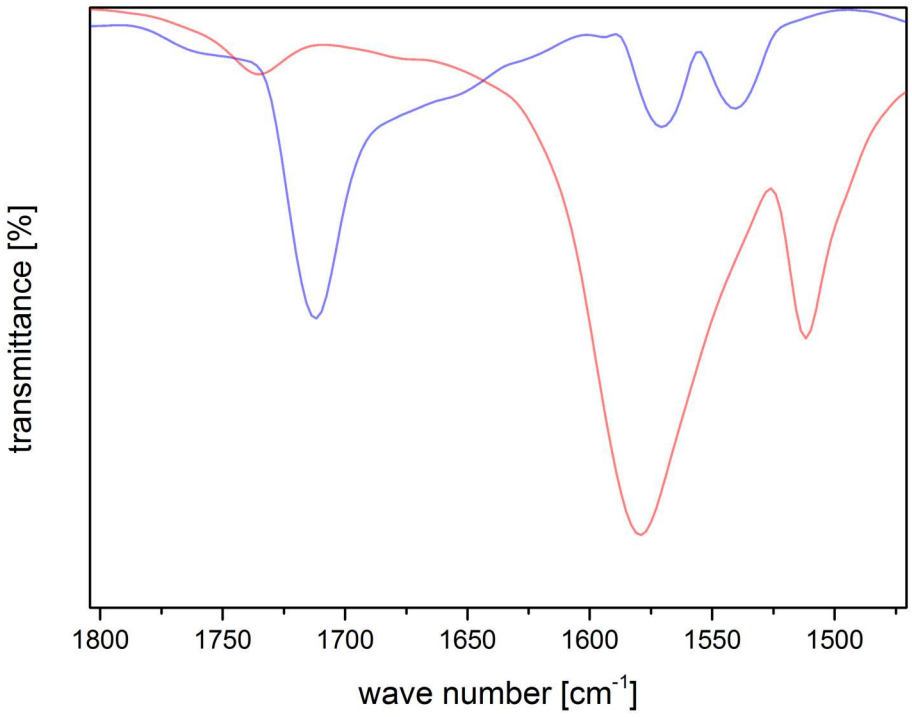

Figure 11: *comparison of IR-spectra of* ***8*** *(blue) and* ***8a*** *(red) in the range of 1800 to 1450 cm^{-1}*

The assignment of the peaks was done according to literature.[84,85] For the deprotonated species **8a** one can see two significant peaks. The band at 1579 cm^{-1} correlates with the carboxylate group and the band at 1512 cm^{-1} which could be the C=C valence stretching vibration. For compound **8** the most prominent band can be seen at 1712 cm^{-1} which relates to the carboxylic acid. Again, the possible C=C valence stretching vibration can be observed for compound **8** but this time at higher wave numbers at 1540 cm^{-1}. Furthermore, the band at 1571 cm^{-1} could correlate again with the presence of a carboxylate group, but as it can be seen at a lower intensity than in the case of **8a**. Or it could correlate with ring C=C and N=C-N stretching vibrations of the imidazole. The results of the comparisons of the ^{1}H-NMR as well as the IR-spectra might suggest that the more probable structure of compound **8** is as proposed the protonated one.

A general scheme of these saponification reactions is depicted in Scheme 4.

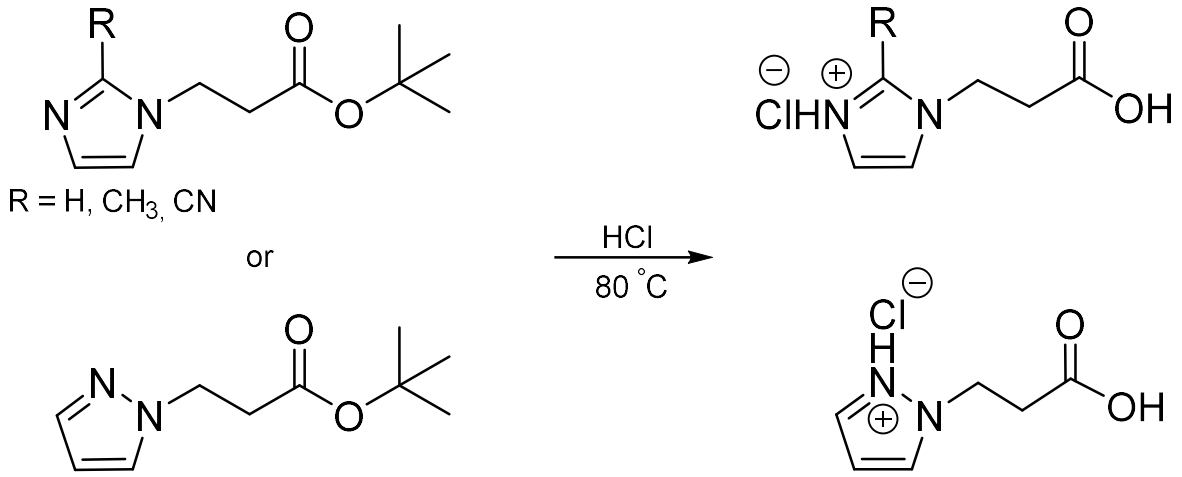

Scheme 4: *general reaction procedure of saponification reactions*

These saponification reactions usually took between 15 to 24 h to reach solidification and gave **8** to **11** in 92 to >99% yield. An overview of reaction time and obtained yield of products **8** to **11** is presented in Table 4 below.

Table 4: *overview of reaction time and yield of the synthesis of compound **8** to **11***

compound	N-heterocycle	reaction time [h]	yield [%]
8	imidazole	22	>99
9	pyrazole	18	92
10	2-methylimidazole	24	94
11	2-cyanoimidazole	15	98

All the compounds could be obtained in excellent yields above 90% and only differed in the reaction time until solidification occurred and stirring was not possible anymore. For the characterization of said compounds **8** to **11** the disappearance of the tert-butyl group in the NMR spectra was tracked. An exemplary ^{1}H-NMR spectrum of 1-(2-carboxyethyl)-1H-imidazol-3-ium chloride, with which the general characterization of said compounds is explained, is presented in Figure 12.

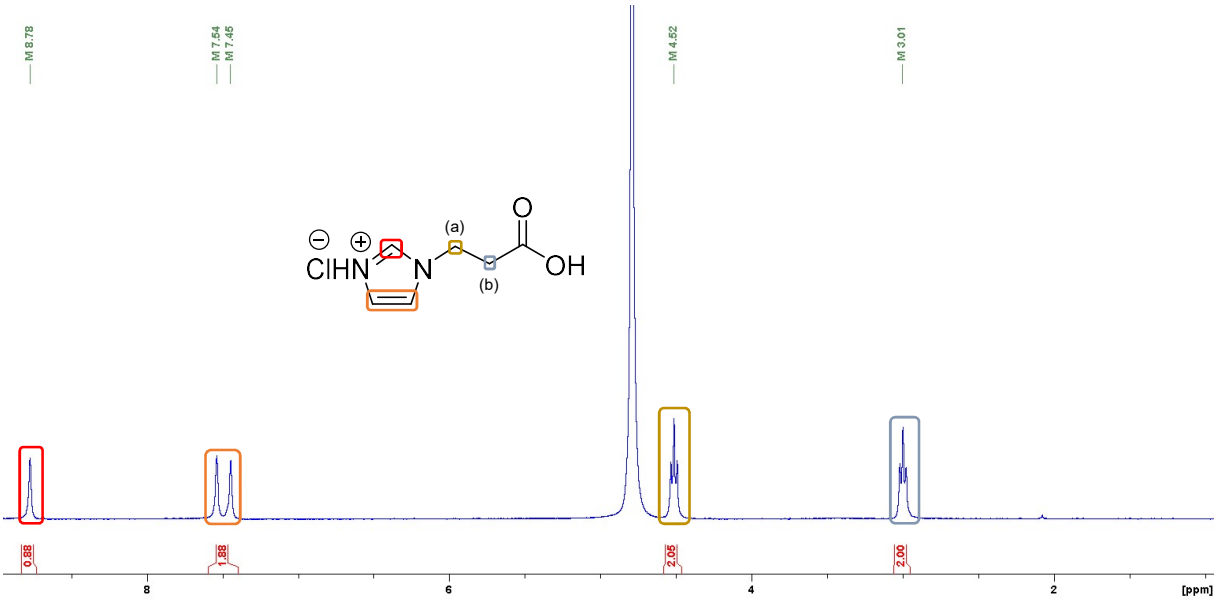

Figure 12: *^{1}H-NMR spectrum of 1-(2-carboxyethyl)-1H-imidazol-3-ium chloride in D_2O*

In comparison with the spectra of the ester derivates the biggest difference is the missing peak of the tert-butyl group which would be expected around 1.40 ppm. The absence of said peak suggests that the reaction reached complete conversion. As before mentioned in chapter 3.1 the shifts of the two ethylene groups differ between the compounds **8** to **11**. A summary of these different shifts is presented in Table 5 below.

Table 5: *summary of ^{1}H-NMR shifts of the two -CH_2 groups of compounds **8** to **11***

compound	N-heterocycle	-CH_2 (a) [ppm]	-CH_2 (b) [ppm]
8	imidazole	4.52	3.01
9	pyrazole	4.60	2.98
10	2-methylimidazole	4.38	2.95
11	2-cyanoimidazole	4.52	3.00

The comparison of the shifts of the two ethylene groups of 1-(2-carboxyethyl)-1H-imidazol-3-ium chloride, **8**, with the two substituted derivates **10** and **11** shows different results.

We cannot observe the same trend as in Table 2 as the EWG of 1-(2-carboxyethyl)-2-cyano-1H-imidazol-3-ium chloride, **11**, shows an almost identical shift of the two ethylene groups as compound **8**. Whereas for 1-(2-carboxyethyl)-2-methyl-1H-imidazol-3-ium chloride, **10**, which has the EDG we see a similar trend as in the case of Table 2 as the $-CH_2$ groups get shifted to lower ppm.

In Figure 13 the exemplary ^{13}C-spectrum of 1-(2-carboxyethyl)-1H-pyrazol-2-ium chloride is presented with which the characterization of the compounds is explained.

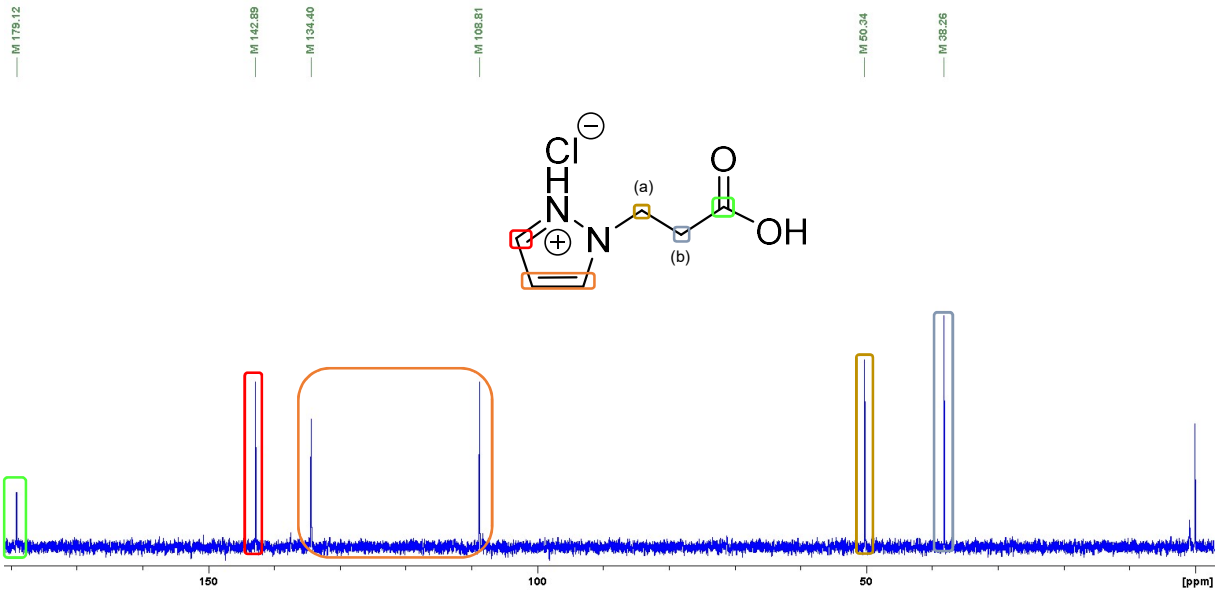

Figure 13: *^{13}C-NMR of 1-(2-carboxyethyl)-1H-pyrazol-2-ium chloride in D_2O with TMS*

In general, the interpretation was done the same way as in the case of Figure 12. Again, one can see that the peak for the tert-butyl group is missing which indicates full conversion. A comparison of the shifts of the ethylene groups of compounds **8** to **11** is presented in Table 6.

Table 6: *summary of ^{13}C-NMR shifts of the two $-CH_2$ groups of compounds **8** to **11***

compound	N-heterocycle	$-CH_2$ (a) [ppm]	$-CH_2$ (b) [ppm]
8	imidazole	45.63	35.74
9	pyrazole	50.34	38.26
10	2-methylimidazole	47.42	39.65
11	2-cyanoimidazole	47.82	40.47

As already discussed with the comparison of the shifts of the ethylene groups in the ^{1}H-NMR spectra seen in Table 5 and Table 2 there can be a similar trend observed when comparing the shifts of said groups in the ^{13}C-spectra summarized in Table 3 and Table 6. In comparison with unsubstituted **8** ethylene groups (a) and (b) experience different shifts in compounds **10** and **11**. It seems that for both groups (a) and (b) the substituted group, whether it is an EDG or EWG, shifts the ethylene groups to higher ppm compared to **8**. This could confirm the hypothesis that a substitution of **8** with an EWG the ethylene groups shift, at least in the ^{13}C-spectra, to higher ppm and when substituted with an EDG to lower ppm.

3.3 Synthesis of metal organic frameworks (MOFs)

After the completion of the saponification reactions compounds **8** to **10** were further reacted with different metal salts. An overview of the used compounds and metal salts is presented in Figure 14 below.

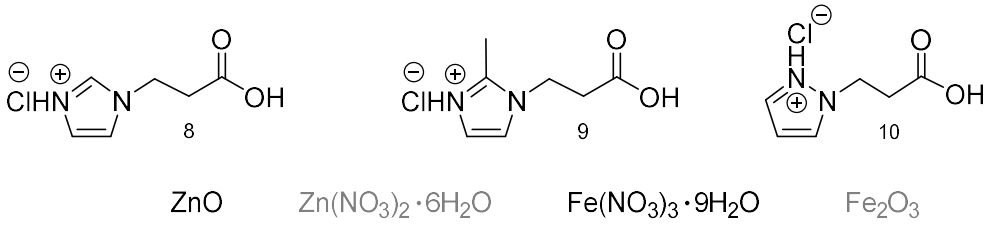

Figure 14: *overview of used organic linkers and metal compounds for the synthesis of MOFs*

The synthetic procedure for the preparation of the MOFs out of compounds **8** to **10** and a metal salt was the following. For the divalent metal ion Zn(II) one equivalent of the corresponding salt was dissolved ($Zn(NO_3)_2$•$6H_2O$) or dispersed (ZnO) in water and a solution of two equivalents of the corresponding ligand in deionized water was prepared. Subsequently the solution of the ligand was added to the metal containing vial and the resulting reaction mixture was heated at 80 °C in a closed vial in a drying oven for at least 24 h, in most cases for some days. For the trivalent iron ions, the same procedure was followed but three equivalents of the ligand were used. The results of the different synthesis are summarized in Table 7 and Table 8. In Table 7 the results of the compounds after the treatment in the oven is summarized whereas in Table 8 the results after removing residual water is presented.

Table 7: *results of the reaction of the metal salts with compounds **8** to **10** after the treatment in the oven; time in oven in brackets*

compound	ZnO	$Zn(NO_3)_2 \cdot 6H_2O$	$Fe(NO_3)_3 \cdot 9H_2O$	Fe_2O_3
8	clear solution (6 days)	clear solution (6 days)	yellow clear solution (6 days)	clear solution with black precipitate (3 days)
9	clear solution (8 days)	clear solution (6 days)	-	-
10	clear solution (1 day)	-	-	-

The results after the additional treatments of the reaction of ligands **8** to **10** with the metal salts is presented in Table 8.

Table 8: *summary of the synthesis of the MOFs out of compound **8** to **10** and the metal compounds with * = special treatment, x = not successful, - = not performed*

compound	ZnO	$Zn(NO_3)_2 \cdot 6H_2O$	$Fe(NO_3)_3 \cdot 9H_2O$	Fe_2O_3
8	colorless gel-like solid	colorless solid*	orange solid	green liquid
9	colorless cloudy solid	yellowish solid*	-	-
10	colorless gel-like solid	-	-	-

Although none of the reaction products could be fully characterized (which should be subject to further investigations), some interesting findings were obtained.

The reaction of $Zn(NO_3)_2 \cdot 6H_2O$ with the ligands **8** and **9** yielded after removal of more than two thirds of water no precipitate. The pH-value of the remaining solution was measured to be between 1 and 2. Upon addition of NaOH a colorless (in case of **8**) or a yellowish (in case of **9**) precipitate immediately formed which is presumably a MOF type compound. IR-measurements of these precipitates were performed and compared to corresponding MOFs obtained by Katharina Kodolitsch in her diploma thesis. The comparison (see Figure 15 in case of **8** and Figure 16 in case of **9**) revealed the presence of yet unknown structures which were not further investigated.

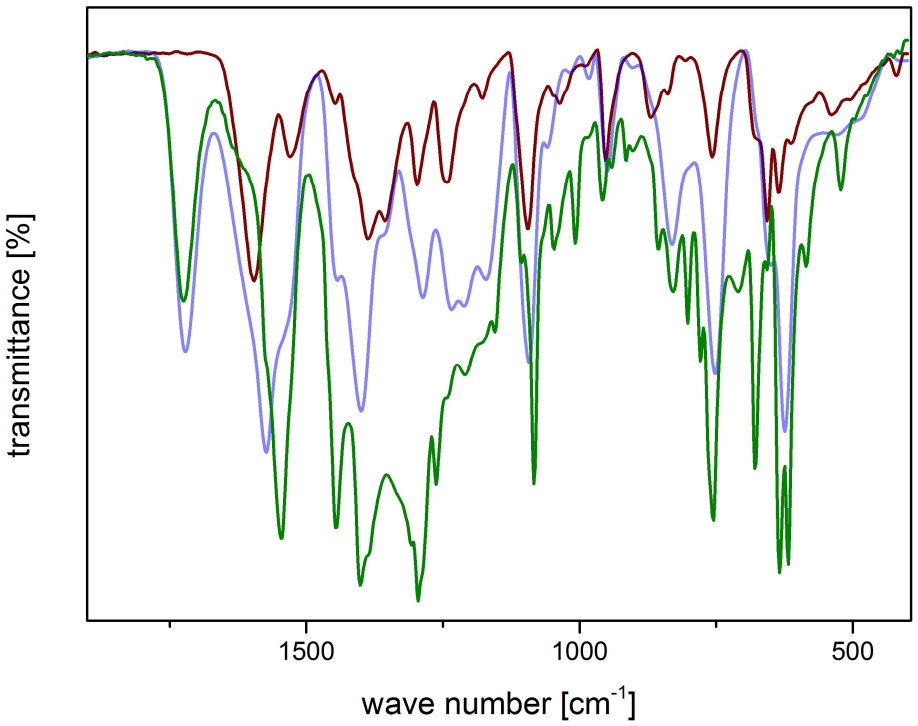

Figure 15: *comparison of* ***8*** *with (green) and without (blue) base treatment compared to the corresponding MOF of Kodolitsch (red) in the range of 1800 to 450 cm^{-1}*

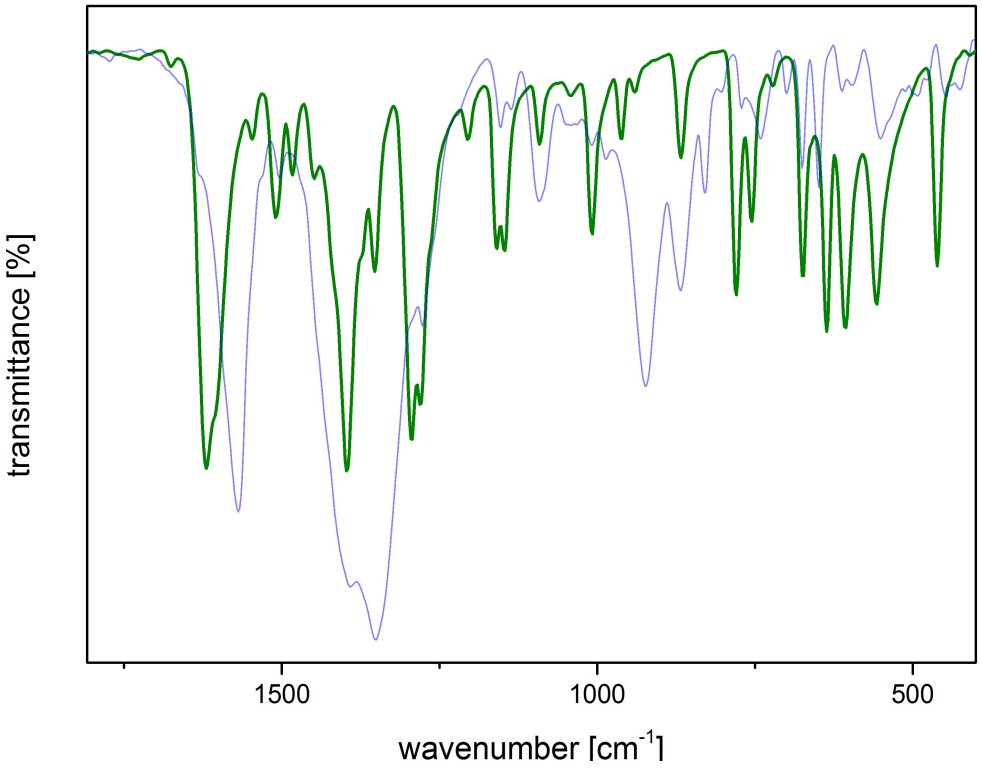

Figure 16: *comparison of* ***9*** *(blue) with the corresponding MOF of Kodolitsch in the range of 1800 to 450 cm^{-1}*

Nonetheless these systems might still be suitable for the base triggered preparation of (most probably up to now not disclosed) MOFs.

The reaction of 1-(2-carboxyethyl)-2-methyl-1H-imidazol-3-ium chloride, **9**, with ZnO yielded after 8 days at 80 °C and 20 days at room temperature an agglomeration of small cloudy colorless crystals seen in Figure 17.

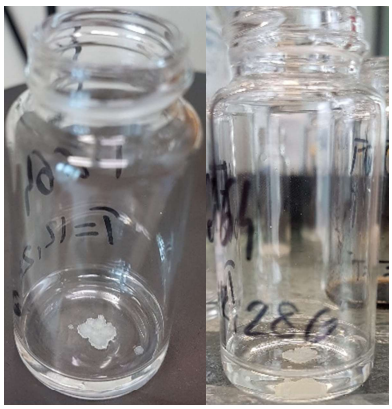

Figure 17: *formed agglomerated crystals of reaction of* ***9*** *with ZnO from different perspectives*

Unfortunately said crystals were not suitable to perform single crystal structure determination. However it is plausible that ZnO has been transformed into a MOF as described by K. Kodolitsch in her master thesis. Accordingly, **9** might be used to transform insoluble ZnO into a MOF. A similar transformation of ZnO with ligand **8** is studied in more detail as follows.

The reaction of **8** (and **10**) with zinc oxide yielded, upon removal of water, colorless oils, which were characterized by NMR and IR spectroscopy. When comparing the ^{1}H-NMR spectrum of said product and unreacted **8** (see Figure 18) it is evident that a reaction took place as all protons of **8** were shifted to higher field.

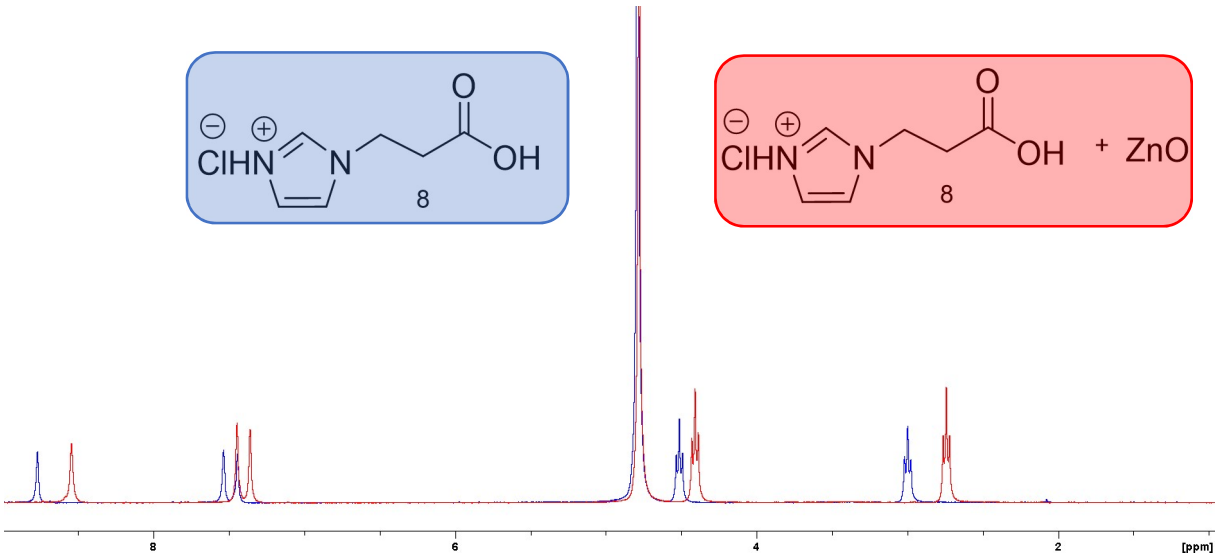

Figure 18: *comparison of ^{1}H-NMR spectra of **8** (blue) and **8**+ZnO (red) in D_2O*

This result suggests that the zinc ion may have coordinated to the ligand, but it is not clear in which manner. To further shed light on the structural nature of the oil its IR spectrum was compared with the IR spectra of MOFs formed by the reaction of ligand **8a** with $Zn(NO_3)_2 \cdot 6H_2O$ as synthesized by Kodolitsch (see Figures 19 and 20).

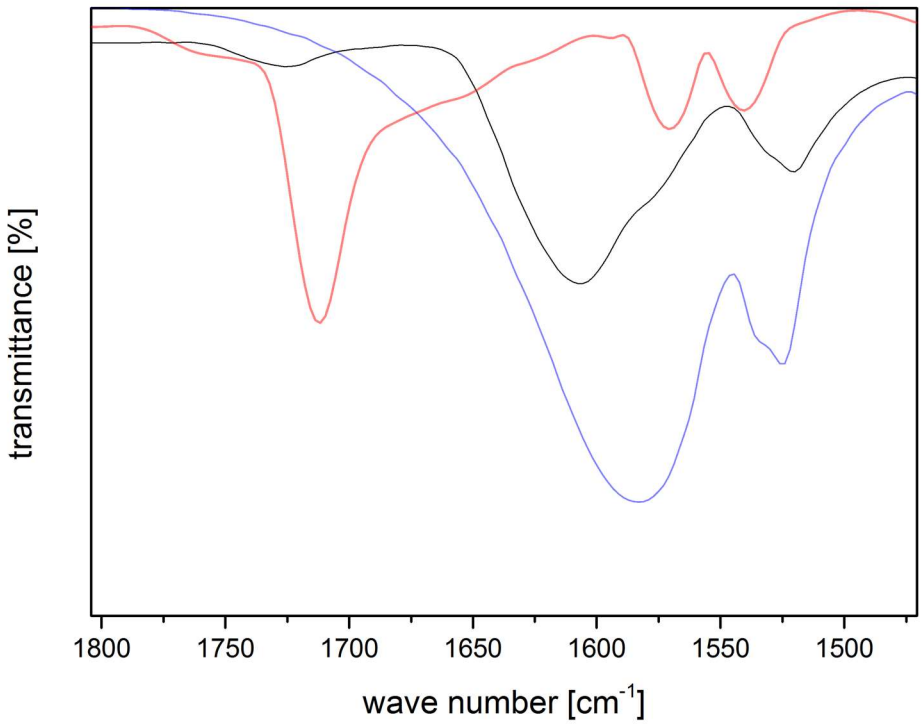

Figure 19: *comparison of IR spectra of **8** (red), **8** reacted with ZnO (blue) and **8a** reacted with $Zn(NO_3)_2 \cdot 6H_2O$ (black) in the range of 1800 to 1450 cm^{-1}*

When comparing the spectrum of **8** and **8** reacted with zinc oxide one can observe the missing of the band correlating with the carboxylic acid and the now present bands at 1583, assigned to a carboxylate group, and 1526 cm^{-1}, assigned to a ring C=C valence stretching vibration. Moreover, both IR spectra look rather similar suggesting a similar coordination mode of the ligand as it has been found in the solid-state structure of crystal retrieved from reacting **8a** with Zn^{2+} (for the structure of the MOF obtained from **8a** and Zn^{2+} see the diploma theses of K. Kodolitsch).

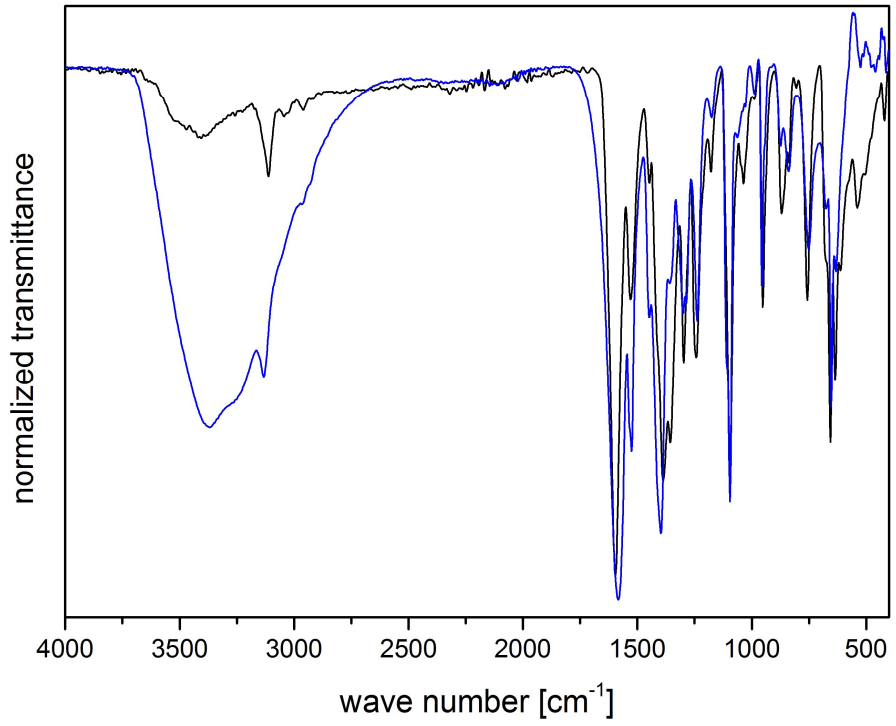

Figure 20: *comparison of IR spectra of **8** reacted with ZnO (blue) and **8a** reacted with $Zn(NO_3)_2 \cdot 6H_2O$ (black) in the range of 4000 to 450 cm^{-1}*

Furthermore, it can be seen that the oil obtained with ligand **8** still has some residual water left which corresponds with the broad band ranging from 3700 to 2700 cm^{-1}. Nonetheless it can be seen that both spectra overlap quite good in the fingerprint region. This leads to the hypothesis that upon reacting compound **8** with zinc oxide and reacting **8a** with $Zn(NO_3)_2 \cdot 6H_2O$ similar MOF like structures may have developed even though their different synthetic routes. To further prove this point TGA measurements of both compounds were made. The comparison of these curves is presented in Figure 21.

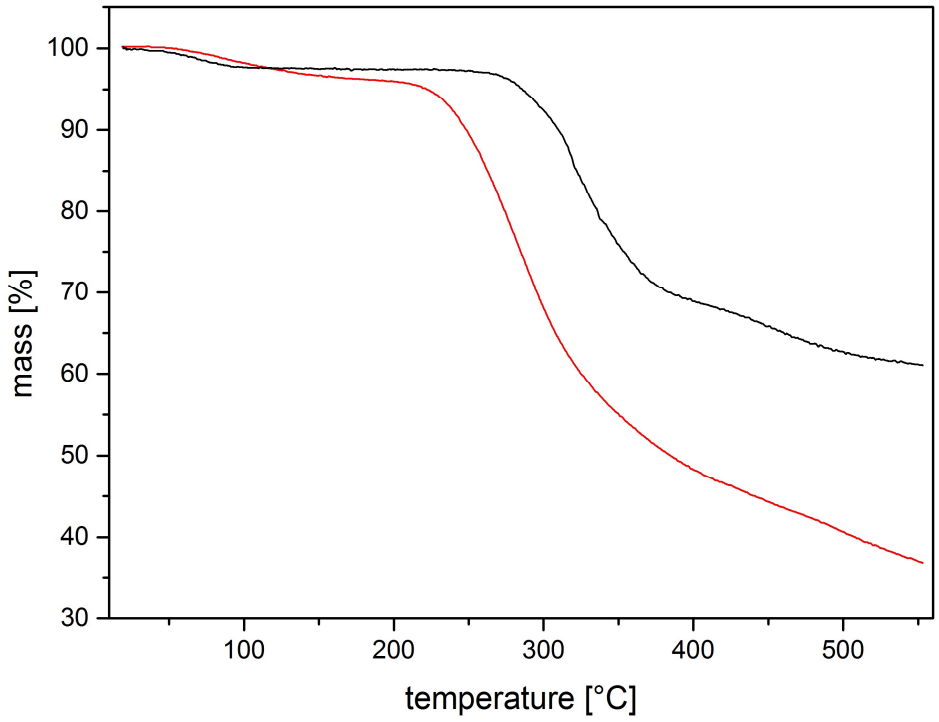

Figure 21: *comparison of TGA measurements of* ***8*** *(red) and* ***8a*** *(black)*

It can be seen that even though the comparison of the IR spectra of **8** reacted with zinc oxide and **8a** reacted with $Zn(NO_3)_2 \cdot 6H_2O$ suggested that a similar compound was formed, the comparison of the TGA curves would suggest otherwise. The overall mass loss of both compounds is summarized in Table 9.

Table 9: *summary of overall mass loss [%] of* ***8*** *and* ***8a***

compound	mass loss [%]
8 + Zn^{2+}	63.08
8a + Zn^{2+}	38.71

The overall mass loss of the reacted compound **8** is significantly higher than that of the reacted **8a**. A similarity which can be seen in both curves is the loss of 1 eq of water at around 100 °C. Otherwise the curves behave differently. This may result in the differences in the appearances of both compounds. Reacted compound **8** is a liquid whereas reacted **8a** is a crystalline substance. Due to these structural differences and the amorphous character of reacted **8** the hypothesis is that both compounds may have a similar chemical constitution but differ in their build. The proposal is that in reacted compound **8** chloride is implemented in the structure which could lead to the higher overall mass loss in comparison to reacted **8a**.

It can be summarized that compound **8 + Zn^{2+}** is an interesting compound for further investigations as it may show porous characteristics in liquid state. Nevertheless, it was shown that **8 + Zn^{2+}** and **8a + Zn^{2+}** are not the same compound. This leads to the hypothesis that the formed product is dependent on the used saponification conditions as **8** was synthesized under acidic and **8a** under basic conditions. But for the further synthesis of tetrazine based organic linkers it was important to establish that an acidic saponification does not harm the carbonitrile group. A more detailed discussion of this topic is presented in chapter 3.4.3.

As iron(III)oxide was not soluble in water it was just suspended in it and added to the in water dissolved 1-(2-carboxyethyl)-1H-imidazol-3-ium chloride, **8**, and subsequently put in the drying oven at 80 °C. After three days the supernatant liquid was removed from the vial and put in a new one which was put out of the drying oven. After a month the remaining liquid was concentrated to such a small volume that only the green liquid and a small amount of undissolved Fe_2O_3 remained. There are still further measurements needed to determine if the resulting solids (and liquids) really can be regarded as coordination polymers.

For the synthesis of the MOF out of **8** and $Fe(NO_3)_3 \cdot 9H_2O$, 3 eq of **8** and 1 eq of iron nitrate nonahydrate were dissolved in deionized water and put together. This resulted in a yellowish cloudy solution which was put in the drying oven at 80 °C. After one week it was put out of said oven to concentrate the remaining liquid to a smaller volume at RT to induce crystal growth. After 3 weeks the remaining liquid was gone, and the reaction yielded two sorts of crystals, orange needles and colorless small rhombuses. For both solid single crystal X-ray diffraction measurements were performed by Dr. Ana Torvisco. In the following, the molecular structure of both crystals is shown – however, it is to note that the quality of the diffraction patterns did not allow for obtaining publishable datasets in both cases.

The colorless needles turned out to be nitrate analogue of ligand **8**, it means, that anion metathesis occurred. Presumably, the weekly coordinating NO_3^- was replaced by the better ligand Cl^- forming Fe(III)-Cl bonds. An illustration of a part of the elemental cell is depicted in Figure 22.

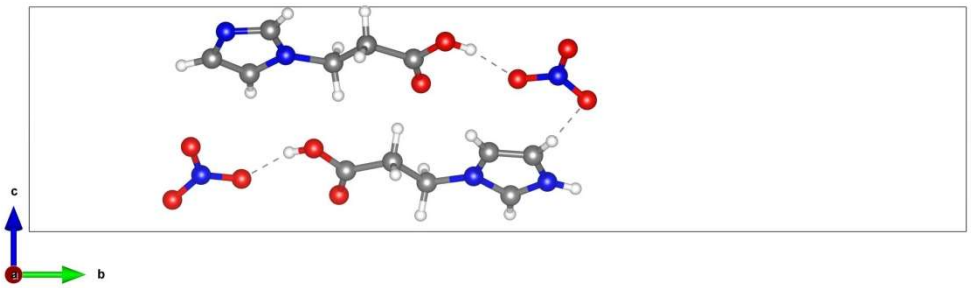

Figure 22: *part of the elemental cell as seen from the a-axis*

The other crystals consist of two, presumably mixed valance, trinuclear iron carboxylate clusters and $FeCl_4^-$ counterions. The imidazolyl group does not coordinate to neither the chloride capped cluster, nor the oxygen (presumably in form of a hydroxo ligand) capped one. Similar iron clusters have been described in literature.[86–90]

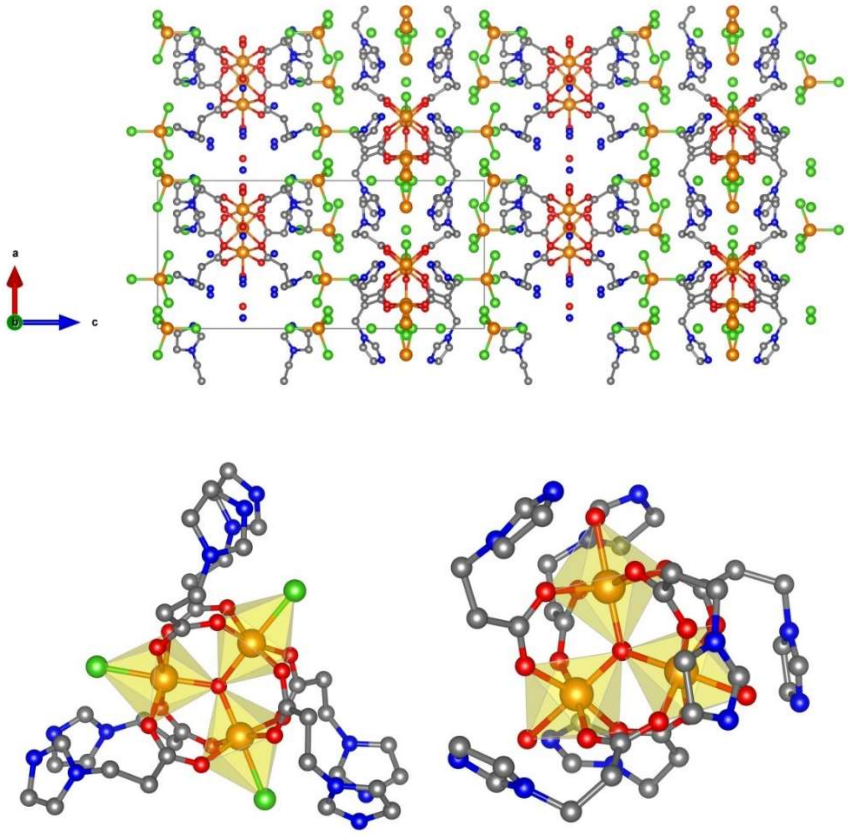

Figure 23: *above, packing of the different molecules seen from the b-axis; below, chloride (left) and oxygen capped iron clusters*

The findings strongly suggest that using ligand **8** as its hydrochloric acid variant will lead to the possibility of the formation of chloride-metal bonds. Accordingly, it is suggested that the ester-cleavage might be better performed with HNO_3 in order to provide a counterion with much weaker coordination capabilities.

3.4 Tetrazine based organic linker

3.4.1 Precursor synthesis

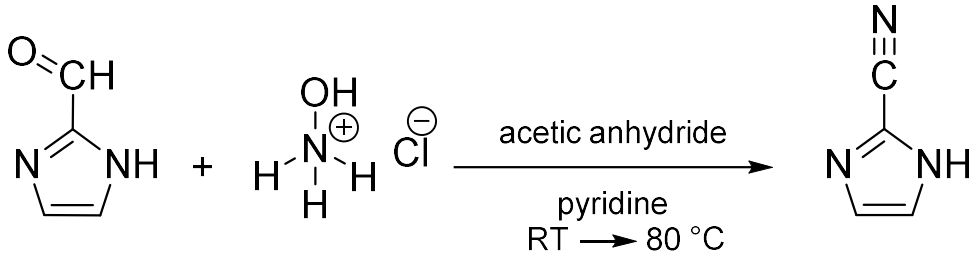

Scheme 5: *synthesis of 1H-imidazole-2-carbonitrile*

For the synthesis of 1H-imidazole-2-carbonitrile the preparation of Trabanco-Suárez et al.[91] was followed. Accordingly, 2-imidazolecarboxaldehyde was suspended in pyridine and hydroxylamine hydrochloride was added portion wise into the stirring suspension. The suspension was then stirred at room temperature for 2 h. Then the mixture was heated to 80 °C and acetic anhydride was added dropwise. After completion the mixture was stirred for another 45 min, which resulted in a clear brown solution. Subsequently it was cooled to 5 °C and basified with NaOH (25%) to pH 8. Afterwards EtOAc was added to dilute the mixture and the organic layer was extracted, dried over sodium sulfate and filtered off, which resulted in a beige solid as a crude product. This crude product was then diluted with DCM and stirred for 72 h, which resulted in a beige solution with beige precipitate. The solid was filtered off and dried under vacuo which resulted in a colorless solid. The overall yield of 1H-imidazole-2-carbonitrile ranged from 38 to 81%. There were various trends observable while performing this synthesis. One trend was that with increasing amount of used 2-imidazolcarboxaldehyde the yield also improved. Another one was observable when switching to a new batch of aldehyde where the yield was significantly improved from around 40 to 81% which is in accordance to literature[91] where a yield of 77% was obtained. Furthermore, a color change of the product from a beige to a colorless solid was observed when switching to the new batch of aldehyde. This could mean that the reaction works better at a bigger scale than a smaller one and that the age of the used aldehyde also significantly influences the overall yield and the color of the product.

For characterization IR-measurements were performed. The assignment of the bands was done according to literature[84,92,85] and a summarization of the most prominent bands is presented in Table 10.

Table 10: *assignment of the IR bands of 1H-imidazole-2-carbonitrile*

wave number [cm^{-1}]	assignment
2235	stretching vibration of cyano group
1653	imidazole I band
1567	ring C=C and N=C-N stretching vibrations
1434	-CHO deformation vibration
1371, 1312	C-N stretching vibration
1116	C-H in plane bending

The broad visible band from 3160 to 2250 cm^{-1} could either result from an (O-H) valence stretching vibration due to residual water left in the compound or from the valence stretching vibration of bonded (N-H) or a combination of both.

Additionally, to the already mentioned Aza-Michael addition with tert-butyl acrylate for this compound to obtain **4** in chapter 3.1. another conjugate addition reaction with methyl acrylate was performed to obtain methyl 3-(2-cyano-1H-imidazol-1-yl)propanoate (**4a**). A comparison of the ^{1}H-NMR spectra of **4** and **4a** is presented in Figure 24.

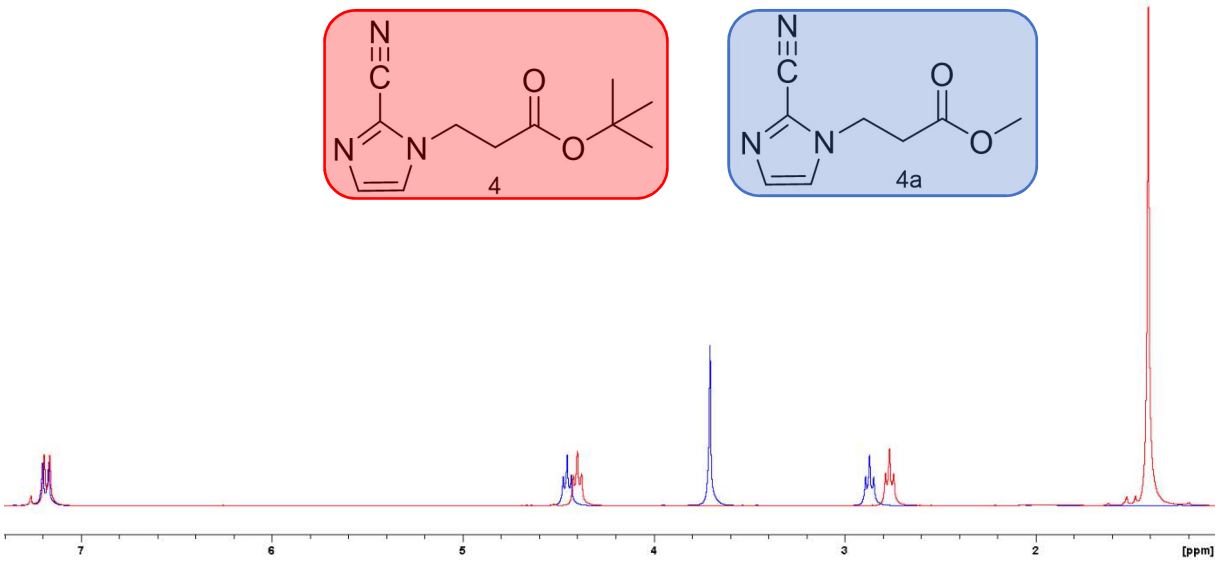

It can be seen that due to the different alkyl groups of the acrylates the formed ethylene bridges experience a different shift. The 1H-imidazole-2-carbonitrile which was alkylated with the tert-butyl acrylate shows a shift to higher field compared to **4a**.

Furthermore, a problem with **4a** occurred when it was tried to saponify said compound under alkaline conditions. Upon saponification the nitrile group was converted via an amide route into a carboxylate group. As the synthetic route to 3,6-symmetrically disubstituted s-tetrazines uses hydrazine as an educt and it is an alkaline compound this may hamper the intended synthesis of organo-soluble tetrazines. Due to this circumstance the focus for the preparation of said compounds shifted to **4**. A more detailed discussion is presented in chapter 3.4.3.

3.4.2 3,6-asymmetrically disubstituted s-tetrazines

The 3,6-asymmetrically disubstituted s-tetrazines were tried to be synthesized following the methods used by Versteegen et al.[93], Kumar et al.[94], Alge et al.[95], Li et al.[96], Zeglis et al.[97] and Yang et al.[98] with slight modifications. In Figure 25 the desired compounds are presented.

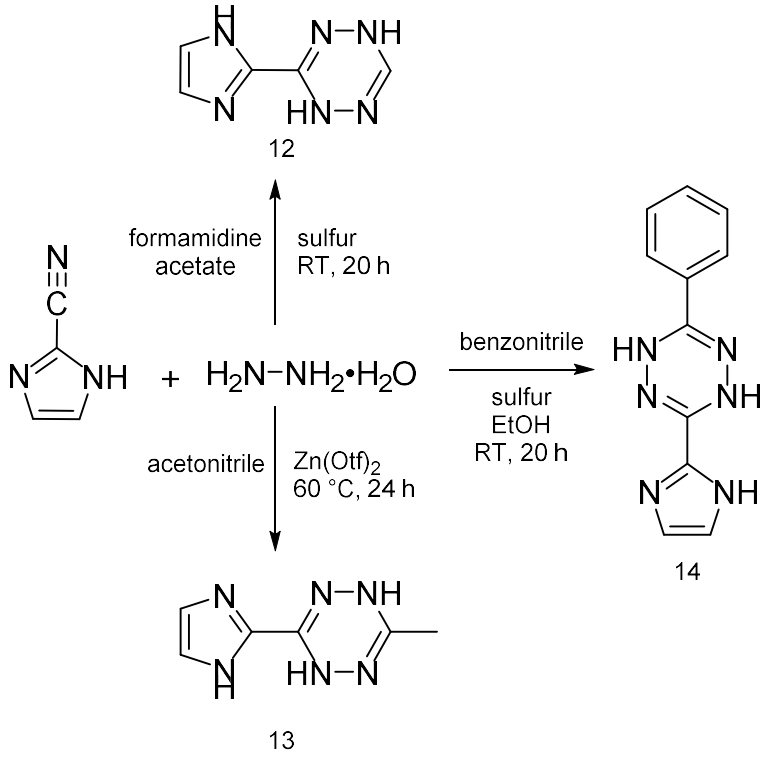

Figure 24: *synthetic approach to 3,6-asymetrically disubstituted s-tetrazines* ***8*** *to****10***

The monosubstituted compound 3-(1H-imidazol-2-yl)-1,4-dihydro-1,2,4,5-tetrazine, **12**, was tried to synthesize following the work instructions of Zeglis et al.[97] with slight modifications. Therefore, hydrazine monohydrate (13 eq) was added to 2-cyanoimidazole (1 eq), formamidine acetate (4 eq) and elemental sulfur (1 eq). 3-(1H-imidazol-2-yl)-6-phenyl-1,4-dihydro-1,2,4,5-tetrazine, **14**, was tried to synthesize following the instructions of Li et al.[96].

Thus, hydrazine monohydrate (10 eq) was added to a suspension of 2-cyanoimidazole (1 eq), benzonitrile (1 eq) and sulfur (4 eq) in EtOH. Following the work instructions of Yang et al.[98], which were slightly modified, it was tried to synthesize 3-(1H-imidazol-2-yl)-6-methyl-1,4-dihydro-1,2,4,5-tetrazine, **13**. Therefore, hydrazine monohydrate (5 eq) was added to 2-cyanoimidazole (1 eq), acetonitrile (5 eq) and zinc triflate (5 mol%).

The added sulfur in the synthesis for compounds **12** and **14** takes part in the reaction of the hydrazine monohydrate and the nitrile. A proposed mechanism on how the sulfur interacts with these compounds was proposed by Li et al.[96] and is depicted in Figure 26.

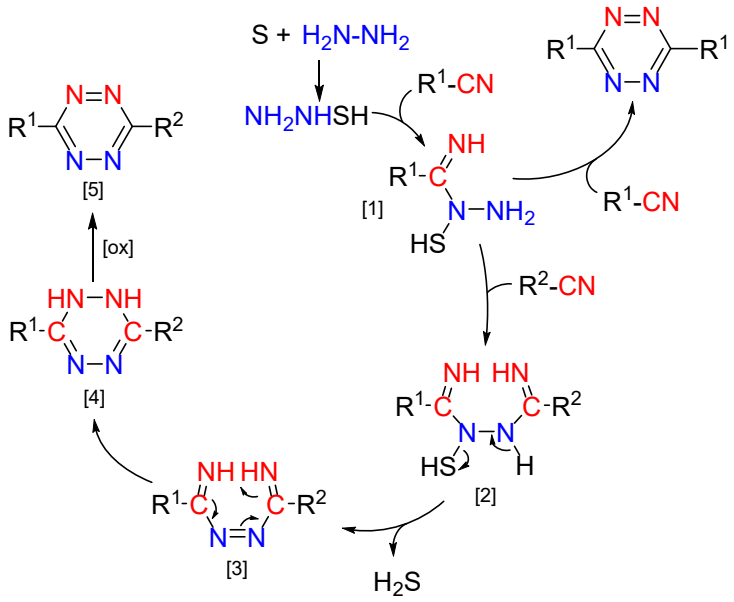

Figure 25: *proposed sulfur induced mechanism for the synthesis of 3,6-asymetrically disubstituted s-tetrazines*[96]

The whole mechanism works via an addition-elimination-rearrangement. The first step is the reaction of sulfur with hydrazine to form mercaptohydrazine, which immediately colors the solution dark red. This is also stated by Han et al..[99] This compound then interacts with the first nitrile, R^1-CN, to form the intermediate species [1]. This compound can now undergo two reactions: either it reacts with the second nitrile, R^2-CN, to form [2] or it can react again with the first nitrile to form the symmetrical product. Nevertheless, the symmetrical product occurs in low yields. This may be because after the reaction of mercaptohydrazine with R^1-CN the concentration of this nitrile decreases whereas the concentration of the yet unreacted R^2-CN stays constant. That is why it would be more probable for [1] to react with the nitrile with the higher concentration, R^2-CN, to form the asymmetrically substituted s-tetrazine.

However, if only one nitrile is present the main product will be the symmetrically substituted s-tetrazine. This makes this sulfur induced mechanism also applicable for the synthesis of 3,6-symetrically disubstituted s-tetrazines. Compound [2] might then be triggered to react to [3] by the elimination of hydrogen sulfide. Then [3] undergoes an electrocyclic rearrangement to form the dihydrotetrazine [4]. It is proposed that [4] then might undergo oxidation by exposure to air but we observed that this might not be sufficient enough and that for the oxidation it is still needed to use e.g. sodium nitrite and acetic acid to form [5].

For the synthesis of **13** zinc triflate was used as a catalyst which is proposed to promote the reaction of the nitrile with hydrazine to form an amidrazone.[98] The promotion may occur due to two possible reasons. The first one is because metal ions are recognized to activate nitriles to nucleophilic addition.[100,101,102] The second one, proposed by Yang et al.[98], is that the formation of the amidrazone intermediate is promoted due to the metal binding as well to the nitrile as to the hydrazine. A possible scheme of this catalytic character of the metal is depicted in Figure 27 below.

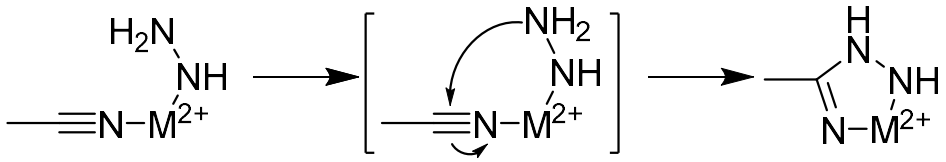

Figure 26: *possible catalytical involvement of the metal during the amidrazone formation*[98]

Upon formation of the dihydrotetrazine the compounds establish their yellow, yellow-orange colors or remain colorless. In contrast their oxidized counterparts, s-tetrazines, show intensive colors like red, violet, red-violet, pink or bluish red.[103,104,105]
A visualization of the synthesis and further oxidation of compound **12** can be seen in the flowchart depicted in Figure 28.

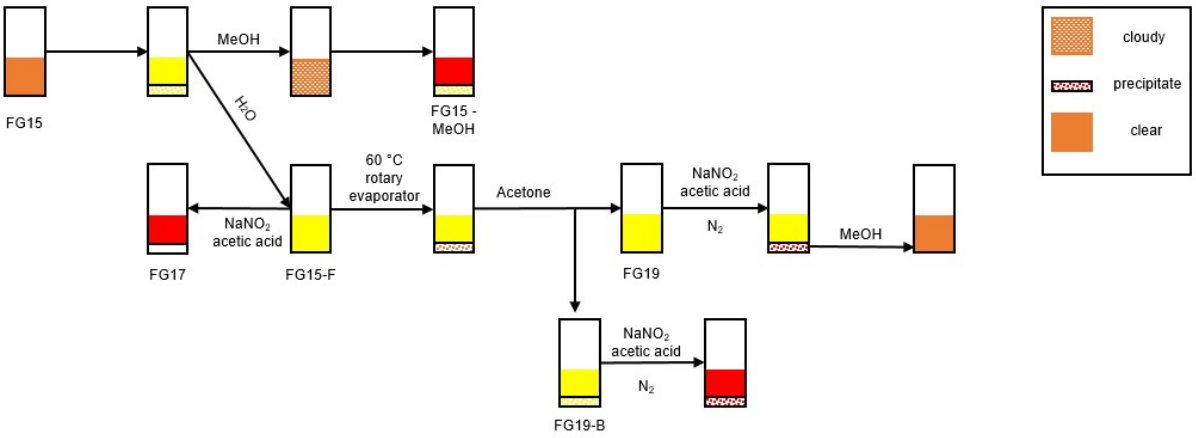

Figure 27: *Flowchart of the tried synthesis of compound **8** and its further oxidation*

Upon adding hydrazine monohydrate to the mixture of 2-cyanoimidazole, formamidine acetate and sulfur the color of the solution immediately turns orange. After 24 h the solution changed its color to yellow and a yellow precipitate was formed. The yellow solid was filtered off and washed with water FG15-F. The solid was then further treated with MeOH which resulted in a cloudy orange solution. This solution changed overnight to a clear red solution with yellow precipitate FG15-MeOH. Part of the yellow filtrate FG15-F was used for an oxidation attempt with sodium nitrite and acetic acid to result in a red clear solution with colorless precipitate. The rest of the filtrate was concentrated to small volume via the use of the rotary evaporator and further dried under reduced pressure which resulted in a clear yellow oily solution with orange precipitate. Subsequently the oxidation of this solution was tried. Therefore, it was partly dissolved in acetone and oxidized with sodium nitrite and acetic acid to obtain either a clear red solution with red precipitate or a clear yellow solution with red precipitate. The obtained red solid was then further treated with MeOH which resulted in an orange clear solution. To sum up it can be said that all the different approaches to synthesize either compound **12** or its oxidized counterpart could have been successful as of their colors but as of their solubility issues it was not possible to characterize them.

A similar procedure was tried to obtain product **13** and its oxidized counterpart. The visualization of this approach is depicted in Figure 29 below.

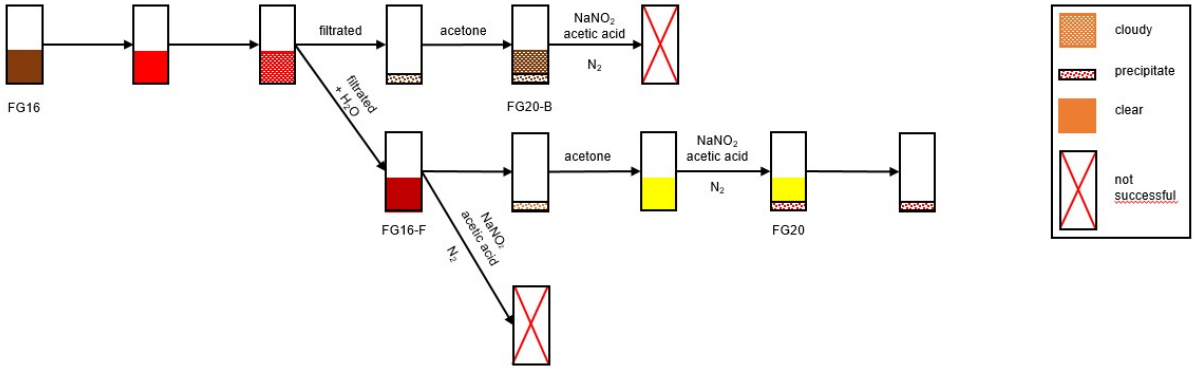

Figure 28: *Flowchart of the tried synthesis of compound* ***13*** *and its further oxidation*

When hydrazine monohydrate was added to the mixture of 2-cyanoimidazole, acetonitrile and zinc triflate a clear brown solution was obtained, which was heated at 60 °C. After 1 h the solution changed to clear red and after another hour the cloudy red solution was obtained. Said solution was then subsequently filtered off and washed with water which obtained the brown solid and the clear red filtrate FG16-F. The solid was then partly dissolved in acetone. This mixture was then tried to be oxidized by sodium nitrite and acetic acid but no color change as visible and the mixture remained cloudy brown with some undissolved brown solid. Part of the red filtrate FG16-F was also tried to be directly oxidized with sodium nitrite and acetic acid but this approach was also not successful because the color did not change. The remaining FG16-F was then dried under reduced pressure to yield an orange solid. The solid was then subsequently dissolved in acetone to obtain a clear yellow solution. This solution was then treated with acetic acid and sodium nitrite in order to oxidize it. This yielded a clear yellow solution with red precipitate. The supernatant was removed and the red solid dried under reduced pressure. As already mentioned before the whole approaches can be summed up that they show promising colors but also the same solubility issues as before. So, compound **13** or its oxidized counterpart could have been synthesized but as of their bad solubility they could not have been characterized.

3.4.3 3,6-symmetrically disubstituted s-tetrazines

For the synthesis of 3,6-symmetrically disubstituted s-tetrazines work instructions of Yang et al.[98] and Li et al.[96] were followed with slight modifications.

In Figure 30 an overview of the desired compounds and their synthetic routes is presented.

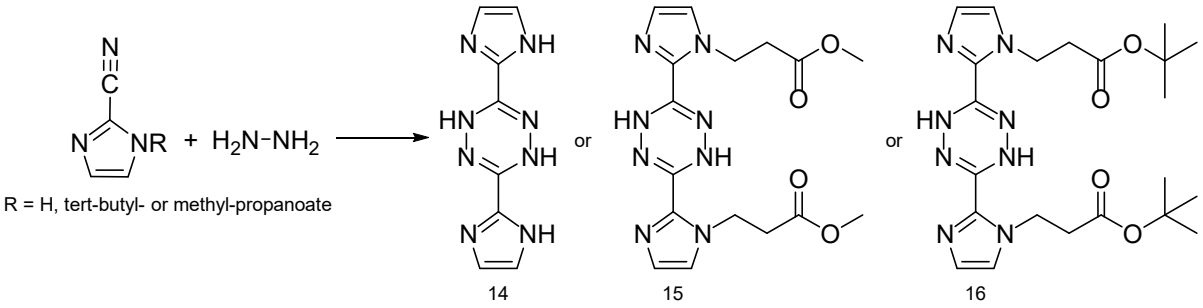

Figure 29: *Synthetic approach to 3,6-symetrically disubstituted s-tetrazines **14** to **16***

Following slightly modified work instructions of Yang et al.[98] it was tried to synthesize 3,6-di(1H-imidazol-2-yl)-1,4-dihydro-1,2,4,5-tetrazine, **14**. Therefore, hydrazine monohydrate was added to 2-cyanoimidazole. This solution was then stirred at 90 °C for 2 h to obtain a yellow foamy solid. The solution was then filtered off and the solid washed with EtOH. Subsequently a yellow solid was obtained which showed poor solubility and it was not possible to characterize **14** according to the ^{1}H-NMR spectrum. As this approach was not successful another one was tried but this time additionally with sulfur. As mentioned in chapter 3.4.2 the addition of sulfur should promote the formation of the tetrazine. Otherwise the procedure stayed the same. Upon adding hydrazine monohydrate to the mixture of 2-cyanoimidazole and sulfur, an orange foam formed. This solution was then stirred at 90 °C for 24 h to obtain a cloudy red solution. The solution was filtered off and a red solid was obtained. Said solid unfortunately showed the same solubility issues as the first approach and therefore it was not possible to characterize compound **14**. Due to these solubility issues compounds **4** and **4a** were synthesized and investigated regarding improvements of said issues. The solubility issue was resolved as both of these compounds were soluble in $CDCl_3$. A problem with compound **4a** was that upon saponification with sodium hydroxide the carbonitrile-group was attacked. This would hamper the potential application of the corresponding dihydro-tetrazine as an organic linker. For the synthesis of **15** hydrazine monohydrate was added to **4a** which resulted in a clear brown solution. Said solution was stirred at 40 °C until a clear yellow solution with yellow precipitate was obtained.

Unfortunately, the yellow precipitate showed poor solubility. Due to these problems the focus shifted to **4**. The hydrolysis reaction of compound **4** is slower than that of **4a** but it was possible to hydrolyse under acidic conditions. Due to that it was possible to maintain the alkaline labile cyano group on compound **4**. Because of these results the focus in further synthesis was shifted to **4** as the used educt for the preparation of the dihydro-tetrazines. Henceforth the synthesis of **16** was done with **4** as carbonitrile instead of the usual 2-cyanoimidazole or **4a**. For the synthesis a hydrazine solution in THF was added to **4** which resulted in a cloudy brown solution. Said solution was stirred at 80 °C for 4 h to obtain a clear orange solution. This time the obtained solution was soluble in $CDCl_3$. Further work up of said compound was done by column chromatography (DCM:MeOH 95:5). A comparison of the ^{1}H-NMR spectra of the unreacted ligand **4** with **16** is presented in Figure 30.

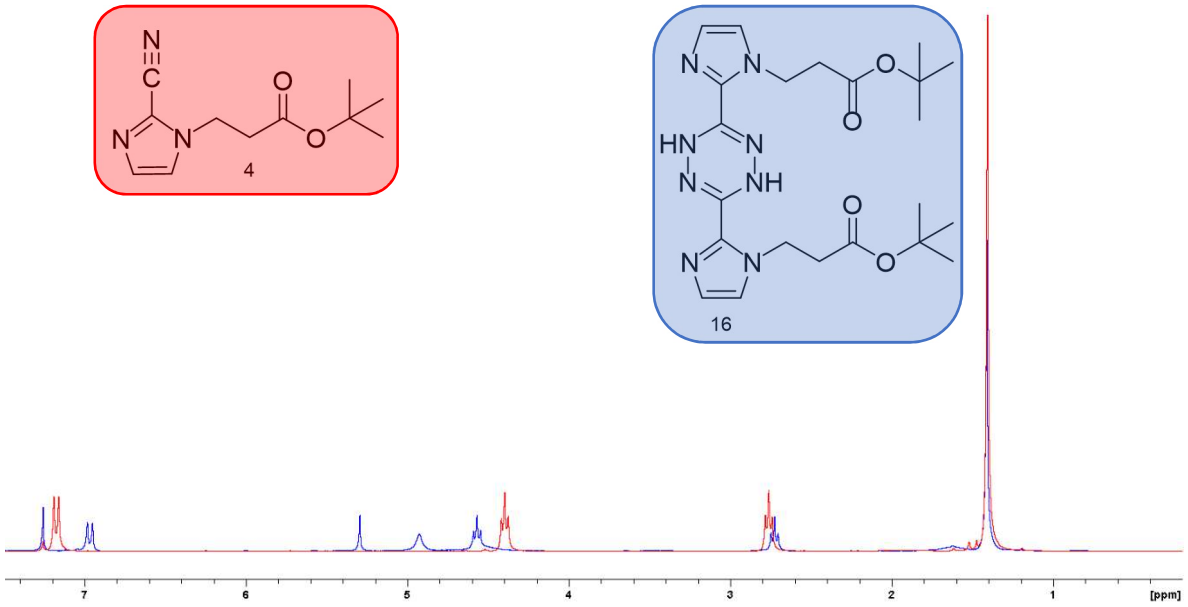

Figure 30: comparison of the ^{1}H-NMR spectra of **4** (red) and **16** (blue)

It can be seen that except for the peak of the tert-butyl group all other peaks experience different shifts upon the reaction with the hydrazine solution. Due to these shifts it is possible that compound **16** was formed but because of the missing signals for the hydrogens of the dihydro-tetrazine it is difficult to confirm.

4 Conclusion and Outlook

Different N-heterocyclic compounds were synthesized and investigated regarding their potential use as linkers in MOFs. Therefore, the parent compounds were alkylated with tert-butyl acrylate and methyl acrylate using a so called aza-Michael addition. The most promising compounds out of these reactions were compounds **1** to **4.** It was determined that for the simultaneous use as ligands for MOFs and as precursor for dihydrotetrazines tert-butyl acrylate is more suitable because it is possible to saponify under acidic conditions as the carbonitrile group is labile to bases. As next step towards potential MOFs the compounds were saponified under acidic conditions which yielded quite pure salts in high yields (>90%).

For the synthesis of MOFs different metal salts out of Zn and Fe were used. The most promising potential MOFs that we were able to synthesize were combinations of Im-linker **8** and Pyr-linker **10** with ZnO which both formed colorless oils. Additionally, also the combination of Im-linker **8** with $Fe(NO_3)_3 \cdot 9H_2O$ showed interesting results as an orange solid was obtained. For the full characterization and confirmation of these MOFs additional measurements are needed.

A new potential precursor to a tetrazine-based organic linker may have been synthesized out of the predesigned N-heterocyclic compound. For this potential linker different catalysts have been tried out resulting that sulfur is the most promising one for synthesis like these. To be certain that the desired compound was synthesized additional measurements are needed. To be used as a linker for MOFs the compound has to be oxidized into the corresponding tetrazine and therefore a suitable synthesis has to be found. If this was successful, the reactivity with different olefins shall be tested and then the linker shall be used in Zn^{2+} and Fe^{3+} MOFs. With these MOFs the iEDDA-reaction as PSM shall be investigated.

5 Experimental

5.1 Chemicals and Instruments

5.1.1 Chemicals

All chemicals have been purchased from Sigma-Aldrich, TCI or ABCR and were, unless specified otherwise, used as received. Used solvents for reactions, workup and purification were of analytical grade and used as received.

For the purification of the synthesized compounds column chromatography was performed. Therefore, silica gel 60 was used as stationary phase. The amount was determined depending on the used column as well as the separation problem which was present.

For thin layer chromatography (TLC), TLC silicagel 60 plates from Merck were used. If spots showed problems with their visibility either an UV-lamp or different dipping solutions were used to make them visible. The two dipping solutions were a potassium permanganate solution and CAM. For the Potassium permanganate solution 1 w% $KMnO_4$ was dissolved in water. For CAM a solution of 10 w% $(NH_3)_3MO_4.4H_2O$ in H_2SO_4 (10 %) was mixed with 10 w% cerium(IV)-sulfate in H_2SO_4 (10%) in a ratio of 12.5 to 1.

5.1.2 Instruments

5.1.2.1 NMR-spectroscopy

The NMR-spectra, ^1H and ^{13}C, were recorded on a Bruker Ultrashield 300. The spectra were obtained in deuterated solvents, $CDCl_3$ and D_2O, at 300.36 MHz for ^1H and 75.53 MHz for ^{13}C. Chemical shifts for the ^1H-spectra are reported in points per million (ppm) relative to the singlet of $CDCl_3$ at 7.26 ppm and relative to the signal of D_2O at 4.79 ppm. The chemical shifts for the ^{13}C-spectra are reported relative to the triplet of $CDCl_3$ at 77.16 ppm and relative to the signal of TMS at 0 ppm for D_2O. The remaining peaks were identified according to literature. The shape of the occurring peaks is specified as follows: s (singlet), d (doublet), t (triplet), m (multiplet).

5.1.2.2 ATR-IR-spectroscopy

The infrared-spectroscopy measurements were taken on an Alpha FT-IR spectrometer from Bruker with the Platinum ATR single reflection diamond ATR module and the results are presented in cm^{-1}

5.1.2.3 Thermogravimetric analysis (TGA)

The TGA measurements were performed by Josefine Hobisch on a Netzsch STA 449 C. The purge and protective gases were helium, with a flow rate of 50 ml/min and as crucible one out of aluminum oxide was used. The temperature range of the experiments ranged from 20 to 550 K with a heating rate of 10 K/min.

5.1.2.4 X-ray crystal structure

The recording of the x-ray crystal structures was done by Ana Torvisco, Ph.D., Institute for inorganic chemistry, on an APEX II diffractometer from Bruker with Mo-K_α radiation.

5.2 Synthesis

5.2.1 1H-imidazole-2-carbonitrile[106]

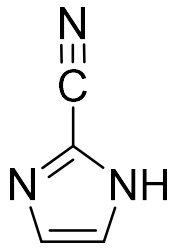

Figure 31: *1H-imidazole-2-carbonitrile*

Chemical formula	$C_4H_3N_3$
Molecular weight	93.09 g/mol
Yield	3.94 g (81.3%)

Hydroxylamine hydrochloride (3.98 g, 57.3 mmol, 1.1 eq) was added to a cooled mixture of 2-imidazolcarboxaldehyde (5 g, 52 mmol, 1 eq) in pyridine (13.93 mL). This mixture was then stirred for 2 h at room temperature. The solution was then heated to 80 °C and acetic anhydride (3.94 mL, 41.6 mmol, 2 eq) was added dropwise over approx. 20 min via a dropping funnel, which resulted in a clear brown solution. Subsequently the mixture was stirred for 45 min. Afterwards it was cooled down to 5 °C and basified with NaOH (25%) to pH 8, clear brown solution. Then EtOAc was added to dilute the mixture and the organic layer was extracted, dried over Na_2SO_4, filtered and the solvent was removed under reduced pressure. This resulted in a beige solid as a crude product. Said crude product was then diluted with DCM and stirred for 72 h, which resulted in a beige solution with beige precipitate. The solid was filtered off and dried under reduced pressure which resulted in a colorless solid.

ATR-IR: v [cm^{-1}]: 2235, 1653, 1567, 1434, 1371, 1312, 1116.

5.2.2 Tert-butyl 3-(2-cyano-1H-imidazol-1-yl)propanoate

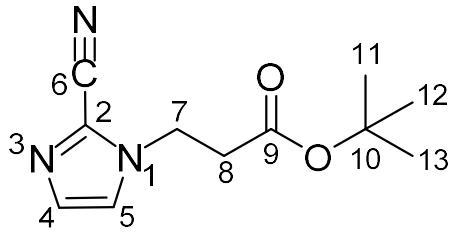

Figure 32: *tert-butyl 3-(2-cyano-1H-imidazol-1-yl)propanoate*

Chemical formula	$C_{11}H_{15}N_3O_2$
Molecular weight	221.26 g/mol
Yield	213 mg (90%)

Tert-butyl acrylate (376 µL, 2.57 mmol, 2.4 eq) was added to 2-cyanoimidazole (100 mg, 1.07 mmol, 1 eq) to form a grey cloudy solution with grey precipitate. This solution was put in the drying oven for 24 h to obtain a clear brown solution. 50 µL of this solution were taken and the unreacted tert-butyl acrylate was removed via N_2 stream over the solution. The resulting brown residue was dissolved in $CDCl_3$ and a NMR spectrum was taken. The remaining mixture was put in the drying oven again for 24 h. This resulted in a clear brown solution.

^{1}H-NMR: ($CDCl_3$, 20 °C, 300.36 MHz): δ [ppm] = 7.19 (s, 1H, Im^5), 7.16 (s, 1H, Im^4), 4.40 (t, $^3J_{HH}$ = 6.37 Hz, 2H, $CH_2CH_2COOC(CH_3)_3$), 2.77 (t, $^3J_{HH}$ = 6.39 Hz, 2H, $CH_2CH_2COOC(CH_3)_3$), 1.41 (s, 9H, $C(CH_3)_3$).

^{13}C{^{1}H}-NMR: ($CDCl_3$, 20 °C, 75.53 MHz): δ [ppm] = 169.15 (1C, C^9), 131.83 (1C, Im^2), 123.86 (1C, Im^5), 121.88 (1C, Im^4), 111.02 (1C, C^6), 82.36 (1C, C^{10}), 43.31 (1C, C^7), 36.48 (1C, C^8), 28.09 (3C, $C^{11,12,13}$).

ATR-IR: v [cm^{-1}]: 2240, 1728, 1152, 906, 727.

5.2.3 Tert-butyl 3-(2-methyl-1H-imidazol-1-yl)propanoate

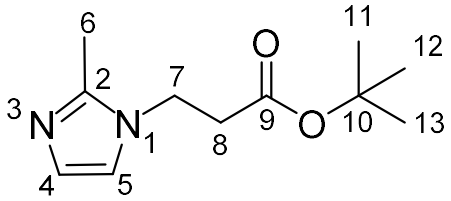

Figure 33: *tert-butyl 3-(2-methyl-1H-imidazol-1-yl)propanoate*

Chemical formula	$C_{11}H_{18}N_2O_2$
Molecular weight	210.28 g/mol
Yield	238 mg (92.6%)

Tert-butyl acrylate (429 µL, 2.93 mmol, 2.4 eq) was added to 2-methylimidazole (101 mg, 1.23 mmol, 1 eq) to form a clear colorless solution with colorless precipitate. This solution was put in the drying oven for 24 h at 80 °C to obtain a clear colorless solution. 50 µL of this solution were taken and the unreacted tert-butyl acrylate was removed via N_2 stream over the solution. The resulting colorless residue was dissolved in $CDCl_3$ and a NMR spectrum was taken. The remaining mixture was put in the drying oven again for 24 h. This resulted in a clear colorless solution.

^{1}H-NMR: ($CDCl_3$, 20 °C, 300.36 MHz): δ [ppm] = 6.86 and 6.82 (s, 2H, $Im^{4,5}$), 4.08 (t, $^3J_{HH}$ = 6.81 Hz, 2H, $CH_2CH_2COOC(CH_3)_3$), 2.61 (t, $^3J_{HH}$ = 6.79 Hz, 2H, $CH_2CH_2COOC(CH_3)_3$), 2.37 (s, 3H, Im^2), 1.39 (s, 9H, $C(CH_3)_3$).

^{13}C{^{1}H}-NMR: ($CDCl_3$, 20 °C, 75.53 MHz): δ [ppm] = 169.86 (1C, C^9), 144.51 (1C, Im^2), 127.36, 119.08 (2C, $Im^{4,5}$), 81.72 (1C, C^{10}), 41.66 (1C, C^7), 36.65 (1C, C^8), 28.11 (3C, $C^{11,12,13}$), 13.10 (1C, C^6).

5.2.4 Tert-butyl 3-(1H-imidazol-1-yl)propanoate[107]

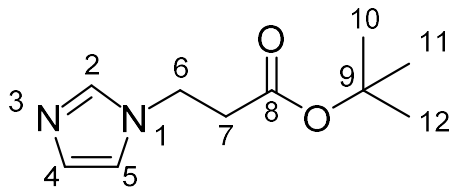

Figure 34: *tert-butyl 3-(1H-imidazol-1-yl)propanoate*

Chemical formula	$C_{10}H_{16}N_2O_2$
Molecular weight	196.25 g/mol
Yield	286 mg (99.3%)

Tert-butyl acrylate (258 µL, 1.76 mmol, 1.2 eq) was added to 1H-Imidazole (100 mg, 1.47 mmol, 1 eq) to form a clear colorless solution with colorless precipitate. This solution was put in the drying oven for 3 h at 80 °C to obtain a clear colorless solution. 50 µL of this solution were taken and the unreacted tert-butyl acrylate was removed via N_2 stream over the solution. The resulting colorless residue was dissolved in $CDCl_3$ and a NMR spectrum was taken. The remaining mixture was put in the drying oven again for 8 h. This resulted in a clear colorless solution.

^{1}H-NMR: ($CDCl_3$, 20 °C, 300.36 MHz): δ [ppm] = 7.52 (s, 1H, Im^2), 7.04 and 6.93 (s, 2H, $Im^{4,5}$), 4.22 (t, $^3J_{HH}$ = 6.42 Hz, 2H, $CH_2CH_2COOC(CH_3)_3$), 2.68 (t, $^3J_{HH}$ = 6.47 Hz, 2H, $CH_2CH_2COOC(CH_3)_3$), 1.43 (s, 9H, $C(CH_3)_3$).

^{13}C{^{1}H}-NMR: ($CDCl_3$, 20 °C, 75.53 MHz): δ [ppm] = 169.89 (1C, C^8), 137.37 (1C, Im^2), 129.61 and 119.05 (2C, $Im^{4,5}$), 81.87 (1C, C^9), 42.75 (1C, C^6), 37.30 (1C, C^7), 28.25 (3C, $C^{10,11,12}$).

5.2.5 Tert-butyl 3-(1H-pyrazol-1-yl)propanoate

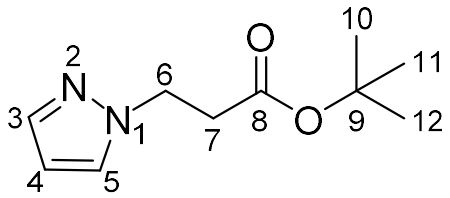

Figure 35: *tert-butyl 3-(1H-pyrazol-1-yl)propanoate*

Chemical formula	$C_{10}H_{16}N_2O_2$
Molecular weight	196.25 g/mol
Yield	210 mg (72.8%)

Tert-butyl acrylate (258 µL, 1.76 mmol, 1.2 eq) was added to pyrazole (103 mg, 1.51 mmol, 1 eq) to form a clear colorless solution with undissolved pyrazole. This solution was put in the drying oven for 3 h at 80 °C to obtain a clear colorless solution. 50 µL of this solution were taken and the unreacted tert-butyl acrylate was removed via N_2 stream over the solution. The resulting colorless residue was dissolved in $CDCl_3$ and a NMR spectrum was taken. The remaining mixture was put in the drying oven again for 8 h. This resulted in a clear colorless solution.

^{1}H-NMR: ($CDCl_3$, 20 °C, 300.36 MHz): δ [ppm] = 7.49 (s,1H, Pyr^5), 7.42 (s, 1H, Pyr^3), 6.20 (s, 1H, Pyr^4) 4.38 (t, $^3J_{HH}$ = 6.67 Hz, 2H, $CH_2CH_2COOC(CH_3)_3$), 2.79 (t, $^3J_{HH}$ = 6.64 Hz, 2H, $CH_2CH_2COOC(CH_3)_3$), 1.43 (s, 9H, $C(CH_3)_3$).

^{13}C{^{1}H}-NMR: ($CDCl_3$, 20 °C, 75.53 MHz): δ [ppm] = 170.53 (1C, C^8), 139.72, 129.78 and 105.44 (3C, $Pyr^{3,4,5}$), 81.40 (1C, C^9), 47.80 (1C, C^6), 36.40 (1C, C^7), 28.20 (3C, $C^{10,11,12}$).

5.2.6 Tert-butyl 3-(1H-1,2,4-triazol-1-yl)propanoate

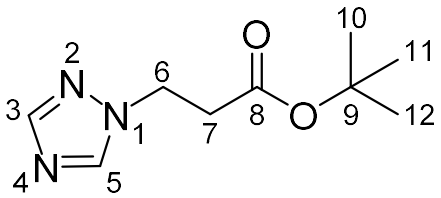

Figure 36: *tert-butyl 3-(1H-1,2,4-triazol-1-yl)propanoate*

Chemical formula	$C_9H_{15}N_3O_2$
Molecular weight	197.24 g/mol
Yield	103 mg (35.9%)

Tert-butyl acrylate (255 µL, 1.74 mmol, 1.2 eq) was added to 1,2,4-triazole (104 mg, 1.47 mmol, 1 eq) to form a clear colorless solution with undissolved 1,2,4-triazole. This solution was put in the drying oven for 48 h at 80 °C. 50 µL of this solution were taken and the unreacted tert-butyl acrylate was removed via N_2-stream over the solution. The resulting residue was dissolved in $CDCl_3$ and a NMR spectrum was taken. The remaining mixture was put in the drying oven again for 4 d. This resulted in a clear colorless solution with colorless precipitate. This solution was dried under vacuum to obtain colorless crystals.

^{1}H-NMR: ($CDCl_3$, 20 °C, 300.36 MHz): δ [ppm] = 8.13 and 7.93 (s, 2H, $Tri^{3,5}$), 4.42 (t, 2H, $^3J_{HH}$ = 6.30 Hz, 2H, $CH_2CH_2COOC(CH_3)_3$), 2.81 (t, $^3J_{HH}$ = 6.32 Hz, 2H, $CH_2CH_2COOC(CH_3)_3$), 1.40 (s, 9H, $C(CH_3)_3$).

5.2.7 Tert-butyl 3-(1H-benzimidazol-1-yl)propanoate

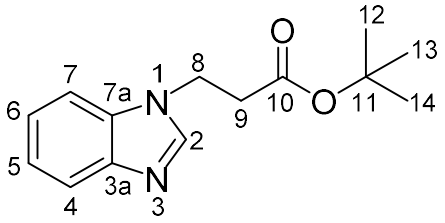

Figure 37: *Tert-butyl 3-(1H-benzimidazol-1-yl)propanoate*

Chemical formula	$C_{14}H_{18}N_2O_2$
Molecular weight	246.31 g/mol
Yield	192 mg (91.8%)

Tert-butyl acrylate (198 µL, 1.35 mmol, 1.6 eq) was added to benzimidazole (99 mg, 0.84 mmol, 1 eq) to form a cloudy colorless solution. This solution was put in the drying oven for 48 h at 80 °C. 50 µL of this solution were taken and the unreacted tert-butyl acrylate was removed via N_2-stream over the solution. The resulting residue was dissolved in $CDCl_3$ and a NMR spectrum was taken. The remaining mixture was put in the drying oven again for 4 d. This resulted in a slightly clouded colorless solution.

^{1}H-NMR: ($CDCl_3$, 20 °C, 300.36 MHz): δ [ppm] = 7.97 (s, 1H, Bzm^2), 7.81 and 7.42 (d, 2H, $Bzm^{4,7}$), 7.30 (m, 2H, $Bzm^{5,6}$), 4.64 (t, 2H, $^3J_{HH}$ = 6.42 Hz, 2H, $CH_2CH_2COOC(CH_3)_3$), 2.79 (t, $^3J_{HH}$ = 6.32 Hz, 2H, $CH_2CH_2COOC(CH_3)_3$), 1.39 (s, 9H, $C(CH_3)_3$).

^{13}C{^{1}H}-NMR: ($CDCl_3$, 20 °C, 75.53 MHz): δ [ppm] = 170.12 (1C, C^{10}), 143.48(1C, Bzm^2) 123.15, 122.29 and 120.76 (3C, $Bzm^{4,5,6}$), 109.59 (1C, Bzm^7) 82.00(1C, C^{11}), 40.76 (1C, C^8), 35.70 (1C, C^9), 28.16 (3C, $C^{11,12,13}$).

5.2.8 Tert-butyl 3-(2-phenyl-1H-imidazol-1-yl)propanoate

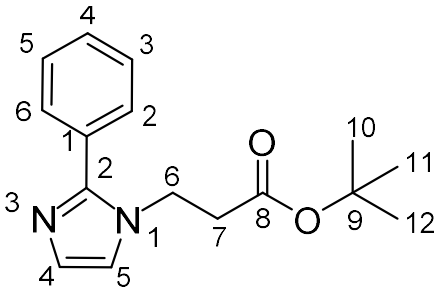

Figure 38: *tert-butyl 3-(2-phenyl-1H-imidazol-1-yl)propanoate*

Chemical formula	$C_{16}H_{20}N_2O_2$
Molecular weight	272.35 g/mol
Yield	152 mg (81.2%)

Tert-butyl acrylate (244 µL, 1.66 mmol, 2.4 eq) was added to phenylimidazole (101 mg, 0.7 mmol, 1 eq) to form a cloudy yellow solution with undissolved phenylimidazole. This solution was put in the drying oven for 48 h at 80 °C. 50 µL of this solution were taken and the unreacted tert-butyl acrylate was removed via N_2 stream over the solution. The resulting residue was dissolved in $CDCl_3$ and a NMR spectrum was taken. The remaining mixture was put in the drying oven again for 4 days. This resulted in a clear yellow solution with colorless precipitate. Said solution was dried under vacuum to obtain a clear yellow oily liquid with a colorless precipitate.

^{1}H-NMR: ($CDCl_3$, 20 °C, 300.36 MHz): δ [ppm] = 7.58 (d, 2H, $Phim^{2,6}$), 7.44 (m, 3H, $Phim^{3,4,5}$), 7.13 and 7.06 (s, 2H, $Im^{4,5}$), 4.30 (t, 2H, $^3J_{HH}$ = 6.93 Hz, 2H, $CH_2CH_2COOC(CH_3)_3$), 2.64 (t, $^3J_{HH}$ = 6.93 Hz, 2H, $CH_2CH_2COOC(CH_3)_3$), 1.41 (s, 9H, $C(CH_3)_3$).

^{13}C{^{1}H}-NMR: ($CDCl_3$, 20 °C, 75.53 MHz): δ (ppm) = 169.90 (1C, C^8), 120.73, 125.50(2C, $Im^{4,5}$), 81.92(1C, C^9), 42.63 (1C, C^6), 37.10 (1C, C^7), 28.23 (3C, $C^{10,11,12}$).

5.2.9 1-(2-carboxyethyl)-2-methyl-1H-imidazol-3-ium chloride

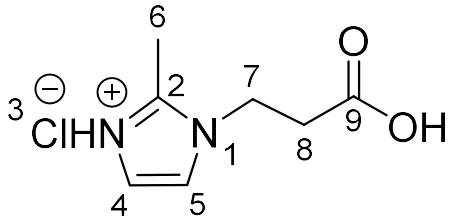

Figure 39: *1-(2-carboxyethyl)-2-methyl-1H-imidazol-3-ium chloride*

Chemical formula	$C_7H_{11}ClN_2O_2$
Molecular weight	190.63 g/mol
Yield	203 mg (94%)

To tert-butyl 3-(2-methyl-1H-imidazol-1-yl)propanoate (238 mg, 1.13 mmol, 1 eq) HCl (6M, 377 µl, 2.26 mmol, 2 eq) was added, which resulted in a clear colorless solution. Said solution was stirred at 80 °C for 24 h to obtain a colorless solid. The obtained solid was dried under reduced pressure.

^{1}H-NMR: (D_2O, 20 °C, 300.36 MHz): δ [ppm] = 7.38 and 7.29 (s, 2H, $Im^{4,5}$), 4.37 (t, $^3J_{HH}$ = 6.19 Hz, 2H, CH_2CH_2COOH), 2.93 (m, 2H, CH_2CH_2COOH), 2.63 (s, 3H, Im^2).

^{13}C{^{1}H}-NMR: (D_2O, 20 °C, 75.53 MHz): δ [ppm] = 181.08 (1C, C^9), 144.29 (1C, Im^2), 123.85, 120.58 (2C, $Im^{4,5}$), 47.42 (1C, C^7), 39.65 (1C, C^8), 12.67 (1C, C^6).

5.2.10 1-(2-carboxyethyl)-1H-imidazol-3-ium chloride

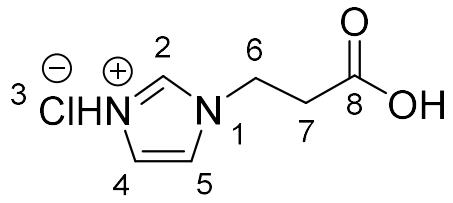

Figure 40: *1-(2-carboxyethyl)-1H-imidazol-3-ium chloride*

Chemical formula	$C_6H_9ClN_2O_2$
Molecular weight	176.60 g/mol
Yield	256 mg (99.3%)

To tert-butyl 3-(1H-imidazol-1-yl)propanoate (286 mg, 1.46 mmol, 1 eq) HCl (6M, 487 µL, 2.92 mmol, 2 eq) was added, which resulted in a clear colorless solution. Said solution was stirred at 80 °C for 24 h to obtain a colorless solid. The obtained solid was dried under reduced pressure.

^{1}H-NMR: (D_2O, 20 °C, 300.36 MHz): δ [ppm] = 8.78 (s, 1H, Im^2) 7.53 and7.44 (s, 2H, $Im^{4,5}$), 4.51 (t, $^3J_{HH}$ = 6.19 Hz, 2H, CH_2CH_2COOH), 2.99 (t, $^3J_{HH}$ = 5.95 Hz, 2H, CH_2CH_2COOH).

^{13}C{^{1}H}-NMR: (D_2O, 20 °C, 75.53 MHz): δ [ppm] = 178.98 (1C, C^8), 137.11 (1C, Im^2), 124.13 and 122.03 (2C, $Im^{4,5}$), 48.22 (1C, C^6), 38.54 (1C, C^7).

5.2.11 1-(2-carboxyethyl)-1H-pyrazol-2-ium chloride

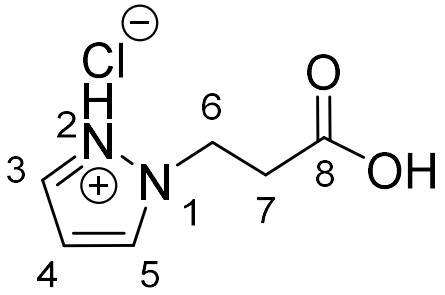

Figure 41: *1-(2-carboxyethyl)-1H-pyrazol-2-ium chloride*

Chemical formula	$C_6H_9ClN_2O_2$
Molecular weight	176.60 g/mol
Yield	173 mg (91.6%)

To tert-butyl 3-(1H-pyrazol-1-yl)propanoate (210 mg, 1.07 mmol, 1 eq) HCl (6M, 357 µL, 2.14 mmol, 2 eq) was added, which resulted in a clear colorless solution. This solution was then stirred at 80 °C for 24 h to obtain a colorless solid. Said solid was then dried under reduced pressure.

^{1}H-NMR: (D_2O, 20 °C, 300.36 MHz): δ [ppm] = 7.97 and 7.89 (s, 2H, $Im^{4,5}$), 6.56 (s, 1H, Im^3) 4.59 (t, $^3J_{HH}$ = 6.20 Hz, 2H, CH_2CH_2COOH), 2.98 (t, $^3J_{HH}$ = 6.24 Hz, 2H, CH_2CH_2COOH).

^{13}C{^{1}H}-NMR: (D_2O, 20 °C, 75.53 MHz): δ [ppm] = 170.79 (1C, C^8), 140.00, 129.55 and 105.44 (3C, $Pyr^{3,4,5}$), 47.64 (1C, C^6), 36.60 (1C, C^7).

5.2.12 1-(2-carboxyethyl)-2-cyano-1H-imidazol-3-ium chloride

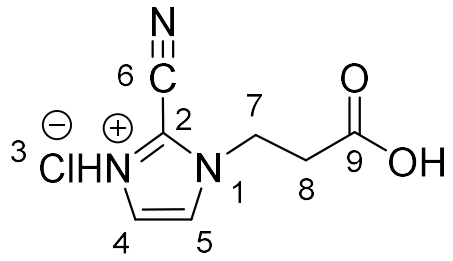

Figure 42: *1-(2-carboxyethyl)-2-cyano-1H-imidazol-3-ium chloride*

Chemical formula	$C_7H_8ClN_3O_2$
Molecular weight	201.61 g/mol
Yield	189 mg (97.7%)

To 2-cyanoimidazole (213 mg, 0.96 mmol, 1 eq) in DCM, HCl (6M, 320 µL, 1.92 mmol, 2 eq) was added which resulted in a clear brown solution. Said solution was stirred at 80 °C overnight to obtain a brownish clear solid. Said solid was then dried under reduced pressure.

^{1}H-NMR: (D_2O, 20 °C, 300.36 MHz): δ [ppm] = 7.53 (s, 1H, Im^4), 7.26 (s, 1H, Im^5), 4.52 (t, $^3J_{HH}$ = 6.23 Hz, 2H, CH_2CH_2COOH), 2.99 (t, 2H, CH_2CH_2COOH)

^{13}C{^{1}H}-NMR: (D_2O, 20 °C, 75.53 MHz): δ [ppm] = 187.62 (1C, C^9), 133.66 (1C, Im^2), 127.53 (1C, Im^5), 47.82 (1C, C^7), 40.47 (1C, C^8).

6 Bibliography

1 S. Kitagawa, R. Kitaura and S. I. Noro, *Angew. Chemie - Int. Ed.*, 2004, **43**, 2334–2375.

2 O. M. Yaghi, M. O'Keeffe, N. W. Ockwig, H. K. Chae, M. Eddaoudi and J. Kim, *Nature*, 2003, **423**, 705–714.

3 C. Janiak, *Dalt. Trans.*, 2003, 2781–2804.

4 D. Bradshaw, J. B. Claridge, E. J. Cussen, T. J. Prior and M. J. Rosseinsky, *Acc. Chem. Res.*, 2005, **38**, 273–282.

5 S. ichiro Noro, S. Kitagawa, T. Akutagawa and T. Nakamura, *Prog. Polym. Sci.*, 2009, **34**, 240–279.

6 J. C. J. Bailar, *Jr. Prep. Inorg. React*, 1964, **1**, 1–27.

7 S. Noro, *Metal-Organic Frameworks*, Elsevier Ltd., 2013, vol. 5.

8 J. B. Decoste and G. W. Peterson, *Chem. Rev.*, 2014, **114**, 5695–5727.

9 G. Férey, C. Serre, C. Mellot-Draznieks, F. Millange, S. Surblé, J. Dutour and I. Margiolaki, *Angew. Chemie - Int. Ed.*, 2004, **43**, 6296–6301.

10 P. L. Llewellyn, S. Bourrelly, C. Serre, Y. Filinchuk and G. Férey, *Angew. Chemie - Int. Ed.*, 2006, **45**, 7751–7754.

11 S. Bourrelly, P. L. Llewellyn, C. Serre, F. Millange, T. Loiseau and G. Férey, *J. Am. Chem. Soc.*, 2005, **127**, 13519–13521.

12 S. Barman, H. Furukawa, O. Blacque, K. Venkatesan, O. M. Yaghi and H. Berke, *Chem. Commun.*, 2010, **46**, 7981–7983.

13 A. R. Millward and O. M. Yaghi, *J. Am. Chem. Soc.*, 2005, **127**, 17998–17999.

14 A. J. Howarth, T. C. Wang, S. S. Al-Juaid, S. G. Aziz, J. T. Hupp and O. K. Farha, *Dalt. Trans.*, 2016, **45**, 93–97.

15 D. Farrusseng, S. Aguado and C. Pinel, *Angew. Chemie - Int. Ed.*, 2009, **48**, 7502–7513.

16 M. Fujita, S. Washizu, K. Ogura and Y. J. Kwon, *J. Am. Chem. Soc.*, 1994, **116**, 1151–1152.

17 O. Ohmori and M. Fujita, *Chem. Commun.*, 2004, **4**, 1586–1587.

18 R. Vaidhyanathan, D. Bradshaw, J. N. Rebilly, J. P. Barrio, J. A. Gould, N. G. Berry and M. J. Rosseinsky, *Angew. Chemie - Int. Ed.*, 2006, **45**, 6495–6499.

19 M. J. Ingleson, J. P. Barrio, J. Bacsa, C. Dickinson, H. Park and M. J. Rosseinsky, *Chem. Commun.*, 2008, 1287–1289.

20 S. Rojas, P. S. Wheatley, E. Quartapelle-Procopio, B. Gil, B. Marszalek, R. E. Morris and E. Barea, *CrystEngComm*, 2013, **15**, 9364–9367.

21 H. Okamoto and M. Yamashita, *Bull. Chem. Soc. Jpn.*, 1998, 71, 2023–2039.

22 A. M. a. Ibrahim, E. Siebel and R. D. Fischer, *Inorg. Chem.*, 1998, **37**, 3521–3525.

23 D. J. Chesnut, D. Plewak and J. Zubieta, *J. Chem. Soc. Dalt. Trans.*, 2001, **3**, 2567–2580.

24 P. J. Hagrman, D. Hagrman and J. Zubieta, *Angew. Chemie - Int. Ed.*, 1999, 2798–2848.

25 S. Banfi, L. Carlucci, E. Caruso, G. Ciani and D. M. Proserpio, *J. Chem. Soc. Dalt. Trans.*, 2002, 2714–2721.

26 J. Zhang, M. M. Matsushita, X. X. Kong, J. Abe and T. Iyoda, *J. Am. Chem. Soc.*, 2001, **123**, 12105–12106.

27 A. D. Burrows, R. W. Harrington, M. F. Mahon and C. E. Price, *J. Chem. Soc. Trans.*, 2000, **2**, 3845–3854.

28 N. Stock and S. Biswas, *Chem. Rev.*, 2012, **112**, 933–969.

29 M. O'Keeffe and O. M. Yaghi, *Chem. Rev.*, 2012, **112**, 675–702.

30 K. K. Tanabe and S. M. Cohen, *Chem. Soc. Rev.*, 2011, **40**, 498–519.
31 S. J. Garibay, Z. Wang, K. K. Tanabe and S. M. Cohen, *Inorg. Chem.*, 2009, **48**, 7341–7349.
32 Z. Wang, K. K. Tanabe and S. M. Cohen, *Inorg. Chem.*, 2009, **48**, 296–306.
33 K. K. Tanabe, Z. Wang and S. M. Cohen, *J. Am. Chem. Soc.*, 2008, **130**, 8508–8517.
34 H. Y. Cho, J. Kim, S. N. Kim and W. S. Ahn, *Microporous Mesoporous Mater.*, 2013, **169**, 180–184.
35 S. S. Kaye, A. Dailly, O. M. Yaghi and J. R. Long, *J. Am. Chem. Soc.*, 2007, **129**, 14176–14177.
36 Tony Boehle, https://commons.wikimedia.org/wiki/File:MIL-53ht.png, https://commons.wikimedia.org/wiki/File:MIL-53ht.png, (accessed 31 July 2018).
37 B. Chen, Z. Yang, Y. Zhu and Y. Xia, *J. Mater. Chem. A*, 2014, **2**, 16811–16831.
38 H. Li, M. Eddaoudi, M. O'Keeffe and O. M. Yaghi, *Nature*, 1999, **402**, 276–279.
39 T. Loiseau, C. Serre, C. Huguenard, G. Fink, F. Taulelle, M. Henry, T. Bataille and G. Férey, *Chem. - A Eur. J.*, 2004, **10**, 1373–1382.
40 C. Serre, F. Millange, C. Thouvenot, M. Noguès, G. Marsolier, D. Louër and G. Férey, *J. Am. Chem. Soc.*, 2002, **124**, 13519–13526.
41 R. Liang, F. Jing, L. Shen, N. Qin and L. Wu, *J. Hazard. Mater.*, 2015, 364–372.
42 M. Eddaoudi, H. L. Li, T. Reineke, M. Fehr, D. Kelley, T. L. Groy and O. M. Yaghi, *Top. Catal.*, 1999, **9**, 105–111.
43 M. Eddaoudi, D. B. Moler, H. Li, B. Chen, T. M. Reineke, M. O'Keeffe and O. M. Yaghi, *Acc. Chem. Res.*, 2001, **34**, 319–330.
44 M. Eddaoudi, J. Kim, N. Rosi, D. Vodak, J. Wachter, M. O. Keeffe, O. M. Yaghi, M. Eddaoudi, J. Kimrn, N. Rosi and O. M. Yaghil, *Science (80-.).*, 2002, **295**, 469–472.
45 H. Chae, J. Kim and Y. Go, *Nature*, 2004, **427**, 523–527.
46 K. Koh, A. G. Wong-Foy and A. J. Matzger, *J. Am. Chem. Soc.*, 2009, **131**, 4184–5.
47 S. H. Jhung, J. Lee and J.-S. Chang, *Bull. Korean Chem. Soc.*, 2005, **26**, 880–881.
48 S. Kaskel, *The Chemistry of Metal-Organic Frameworks*, Wiley-VCH, 2016.
49 M. T. Wharmby, J. P. S. Mowat, S. P. Thompson and P. A. Wright, *J. Am. Chem. Soc.*, 2011, **133**, 1266–1269.
50 S. R. Miller, G. M. Pearce, P. A. Wright, F. Bonino, S. Chavan, S. Bordiga, I. Margiolaki, N. Guillou, G. Férey, S. Bourrelly and P. L. Llewellyn, *J. Am. Chem. Soc.*, 2008, **130**, 15967–15981.
51 T. Devic, P. Horcajada, C. Serre, F. Salles, G. Maurin, D. Heurtaux, G. Clet, A. Vimont, J. Grene, B. Le Ouay, F. Moreau, E. Magnier, Y. Filinchuk, J. Lavalley, M. Daturi, I. Charles and G. Montpellier, *J. Am. Chem. Soc.*, 2008, 1127–1136.
52 G. Férey, *Chem. Soc. Rev.*, 2008, **37**, 191–214.
53 B. Chen, Z. Yang, Y. Zhu and Y. Xia, *J. Mater. Chem. A*, 2014, **2**, 16811–16831.
54 K. S. Park, Z. Ni, A. P. Côté, J. Y. Choi, R. Huang, F. J. Uribe-Romo, H. K. Chae, M. O'Keeffe and O. M. Yaghi, *Proc. Natl. Acad. Sci. U. S. A.*, 2006, **103**, 10186–91.

55 S. A. Moggach, T. D. Bennett and A. K. Cheetham, *Angew. Chemie - Int. Ed.*, 2009, **48**, 7087–7089.

56 A. Phan, C. J. Doonan, F. J. Uribe-Romo, C. B. Knobler, M. O'Keeffe and O. M. Yaghi, *Acc Chem Res*, 2010, **43**, 58–67.

57 H. Hayashi, A. P. Côté, H. Furukawa, M. O'Keeffe and O. M. Yaghi, *Nat. Mater.*, 2007, **6**, 501–506.

58 O. M. Yaghi, *ReVision*, 2008, 939–943.

59 W. Morris, C. J. Doonan, H. Furukawa, R. Banerjee and O. M. Yaghi, *J. Am. Chem. Soc.*, 2008, **130**, 12626–12627.

60 S. S. Chen, *CrystEngComm*, 2016, **18**, 6543–6565.

61 A. Schoedel, Z. Ji and O. M. Yaghi, *Nat. Energy*, 2016, **1**, 16034.

62 C. He, D. Liu and W. Lin, *Chem. Rev.*, 2015, **115**, 11079–11108.

63 M. Eddaoudi, D. F. Sava, J. F. Eubank, K. Adil and V. Guillerm, *Chem. Soc. Rev.*, 2015, **44**, 228–249.

64 Q. Chen, Z. Chang, W. C. Song, H. Song, H. Bin Song, T. L. Hu and X. H. Bu, *Angew. Chemie - Int. Ed.*, 2013, **52**, 11550–11553.

65 Y. X. Sun and W. Y. Sun, *CrystEngComm*, 2015, **17**, 4035–4240.

66 S. K. Callear, M. B. Hursthouse and T. L. Threlfall, *CrystEngComm*, 2010, **12**, 898–908.

67 M. Chen, W. Li, M. Zhang, R. Hu and C. Zhang, 2011, 1175–1178.

68 F. Su, L. Lu, S. Feng and M. Zhu, *CrystEngComm*, 2014, **16**, 7990–7999.

69 P. C. Wang, F. L. Meng, C. Liu, K. Y. Zou and Z. X. Li, *Inorg. Chem. Commun.*, 2012, **17**, 95–98.

70 K. Y. Zou, J. L. Zhao, C. Liu, Z. Wang and Z. X. Li, *Eur. J. Inorg. Chem.*, 2013, 293–298.

71 Y. H. Tan, J. J. Wu, H. Y. Zhou, L. F. Yang and B. H. Ye, *CrystEngComm*, 2012, **14**, 8117–8123.

72 Y. H. Tan, L. F. Yang, M. L. Cao, J. J. Wu and B. H. Ye, *CrystEngComm*, 2011, **13**, 4512–4518.

73 X. L. Zhao and W. Y. Sun, *CrystEngComm*, 2014, **16**, 3247–3258.

74 T. K. Maji, K. Uemura, H. C. Chang, R. Matsuda and S. Kitagawa, *Angew. Chemie - Int. Ed.*, 2004, **43**, 3269–3272.

75 T. Braun, S. P. Foxon, R. N. Perutz and P. H. Walton, *Angew. Chemie - Int. Ed.*, 1999, **38**, 3326–3329.

76 G. Nickerl, I. Senkovska and S. Kaskel, *Chem. Commun.*, 2015, **51**, 2280–2282.

77 S. Razavi, M. Masoomi and A. Morsali, *Inorg. Chem.*, 2017, **56**, 9646–9652.

78 G. Mouchaham, L. Cooper, N. Guillou, C. Martineau, E. Elkaïm, S. Bourrelly, P. L. Llewellyn, C. Allain, G. Clavier, C. Serre and T. Devic, *Angew. Chemie - Int. Ed.*, 2015, **54**, 13297–13301.

79 A. J. Calahorro, A. Peñas-Sanjuan, M. Melguizo, D. Fairen-Jimenez, G. Zaragoza, B. Fernández, A. Salinas-Castillo and A. Rodríguez-Diéguez, *Inorg. Chem.*, 2013, **52**, 546–548.

80 Z. Chang, D. S. Zhang, Q. Chen, R. F. Li, T. L. Hu and X. H. Bu, *Inorg. Chem.*, 2011, **50**, 7555–7562.

81 J. E. Clements, J. R. Price, S. M. Neville and C. J. Kepert, *Angew. Chemie - Int. Ed.*, 2014, **53**, 10164–10168.

82 K. L. Bo, Q. Wu, Q. Q. Xue, S. L. De and F. L. Xian, *Synthesis (Stuttg).*, 2007, 2653–2659.

83 B. Zou and H.-F. Jiang, *Chinese J. Chem.*, 2008, 1309–1314.

84 A. Hesse, *Spektroskopische Methoden in der organischen Chemie*, 2005.
85 G. Socrates, *Infrared and Raman characteristic group frequencies*, 2004.
86 C. Feng, Y. Q. Zhu, X. Y. Xue and H. Zhao, *J. Clust. Sci.*, 2016, **27**, 1181–1190.
87 A. R. Burgoyne, R. Meijboom, A. Muller and B. O. Omondi, *Acta Crystallogr. Sect. E Struct. Reports Online*, 2011, **67**, m1092–m1093.
88 D. Prodius, F. Macaev, E. Stingaci, V. Pogrebnoi, V. Mereacre, G. Novitchi, G. E. Kostakis, C. E. Anson and A. K. Powell, *Chem. Commun.*, 2013, **49**, 2628–2630.
89 E. M. Holt, S. L. Holt, W. F. Tucker, R. O. Asplund and K. J. Watson, *J. Am. Chem. Soc.*, 1974, **96**, 2621–2623.
90 C. P. Guntlin, S. T. Ochsenbein, M. Wörle, R. Erni, K. V. Kravchyk and M. V. Kovalenko, *Chem. Mater.*, 2018, **30**, 1249–1256.
91 WO2012085038A1, 2012.
92 A. Koudijs, P. Lont and H. Van der Plas, *Recueil*, 1971, **90**, 207–212.
93 R. M. Versteegen, R. Rossin, W. Ten Hoeve, H. M. Janssen and M. S. Robillard, *Angew. Chemie - Int. Ed.*, 2013, **52**, 14112–14116.
94 A. Kumar, G. Hao, L. Liu, S. Ramezani, J. T. Hsieh, O. K. Öz and X. Sun, *Bioconjug. Chem.*, 2015, **26**, 782–789.
95 D. L. Alge, D. F. Donohue and K. S. Anseth, *Tetrahedron Lett.*, 2013, **54**, 5639–5641.
96 C. Li, H. Ge, B. Yin, M. She, P. Liu, X. Li and J. Li, *RSC Adv.*, 2015, **5**, 12277–12286.
97 B. M. Zeglis, P. Mohindra, G. I. Weissmann, V. Divilov, S. A. Hilderbrand, R. Weissleder and J. S. Lewis, *Bioconjug. Chem.*, 2011, **22**, 2048–2059.
98 J. Yang, M. R. Karver, W. Li, S. Sahu and N. K. Devaraj, *Angew. Chemie - Int. Ed.*, 2012, **51**, 5222–5225.
99 J. Han, B. Xi, Z. Feng, X. Ma, J. Zhang, S. Xiong and Y. Qian, *Inorg. Chem. Front.*, 2018, **5**, 785–792.
100 V. Y. Kukushkin and A. J. L. Pombeiro, *Chem. Rev.*, 2002, **102**, 1771–1802.
101 Z. P. Demko and K. B. Sharpless, *J. Org. Chem.*, 2001, **66**, 7945–7950.
102 J. Wang, F. Xu, T. Cai and Q. Shen, *Org. Lett.*, 2008, **10**, 445–448.
103 H. Neunhoeffer, *Compr. Heterocycl. Chem.*, 1984, **3**, 531–572.
104 G. Clavier and P. Audebert, *Chem. Rev. (Washington, DC, United States)*, 2010, **110**, 3299–3314.
105 R. J. Brea and N. K. Devaraj, in *Chemoselective and Bioorthogonal Ligation Reactions: Concepts and Applications*, 2017, pp. 67–95.
106 J. P. Whitten, D. P. Matthews and J. R. McCarthy, *J. Org. Chem.*, 1986, **51**, 1891–1894.
107 K. Worm-Leonhard and M. Meldal, *European J. Org. Chem.*, 2008, 5244–5253.

7 List of Figures

8 List of schemes

9 List of tables

10 Appendix

10.1 NMR-spectra

Additional NMR-spectra can be found at: M:\ICTM\ANYONE\Florian Gobec\NMR

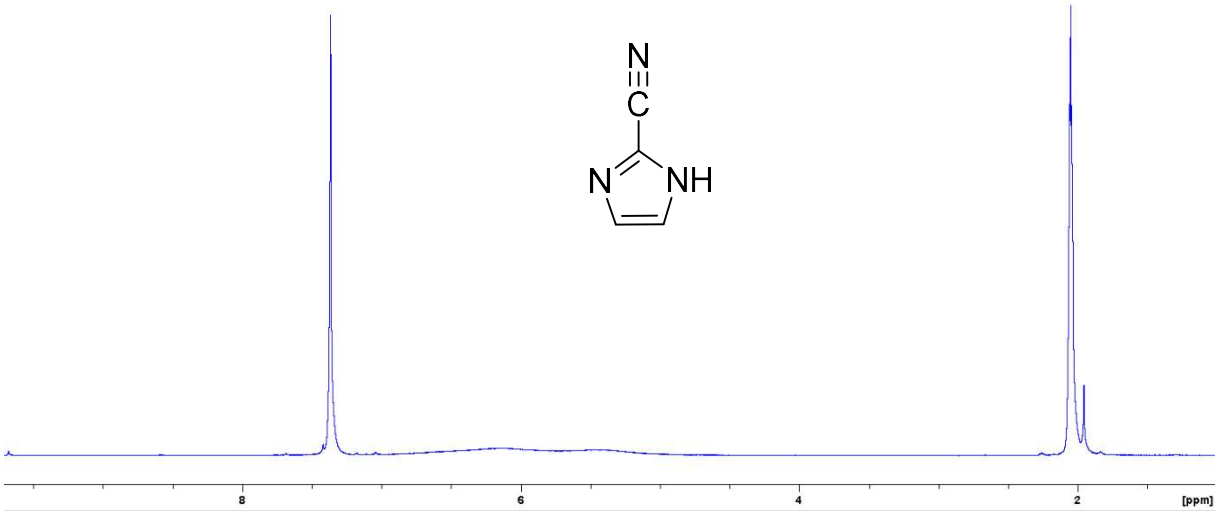

Figure 43: *^{1}H-NMR of 1H-imidazole-2-carbonitrile in acetonde-d_6*
M:\ICTM\ANYONE\Florian Gobec\NMR\FG1

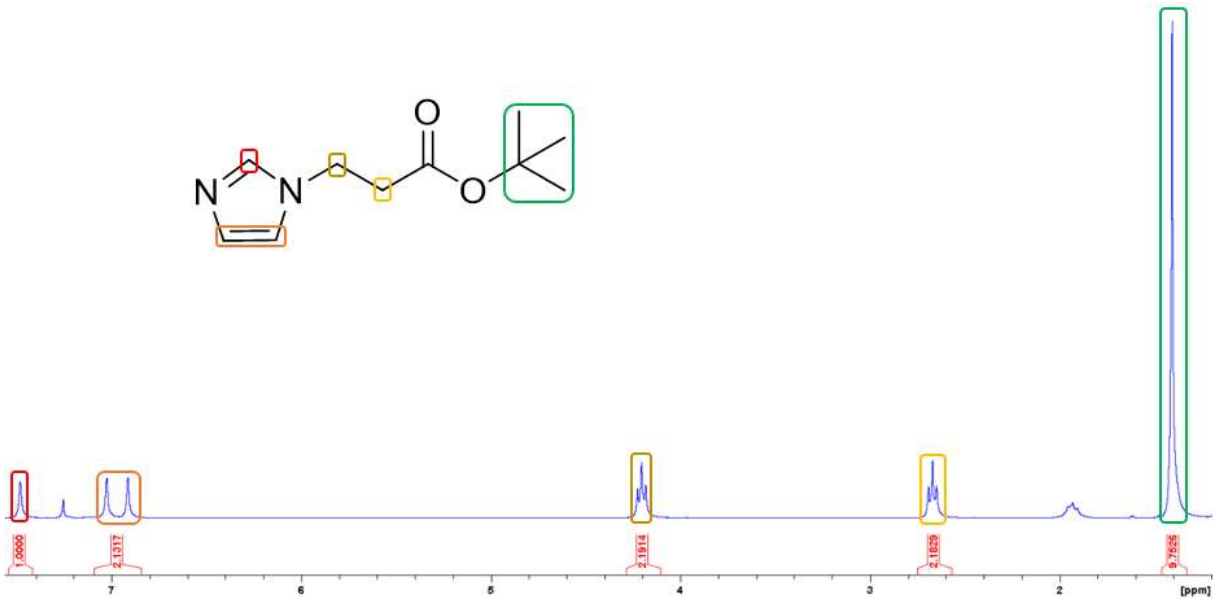

Figure 44: *^{1}H NMR of tert-butyl-3-(1H-imidazol-1-yl)propanoate in $CDCl_3$*
M:\ICTM\ANYONE\Florian Gobec\NMR\FG31

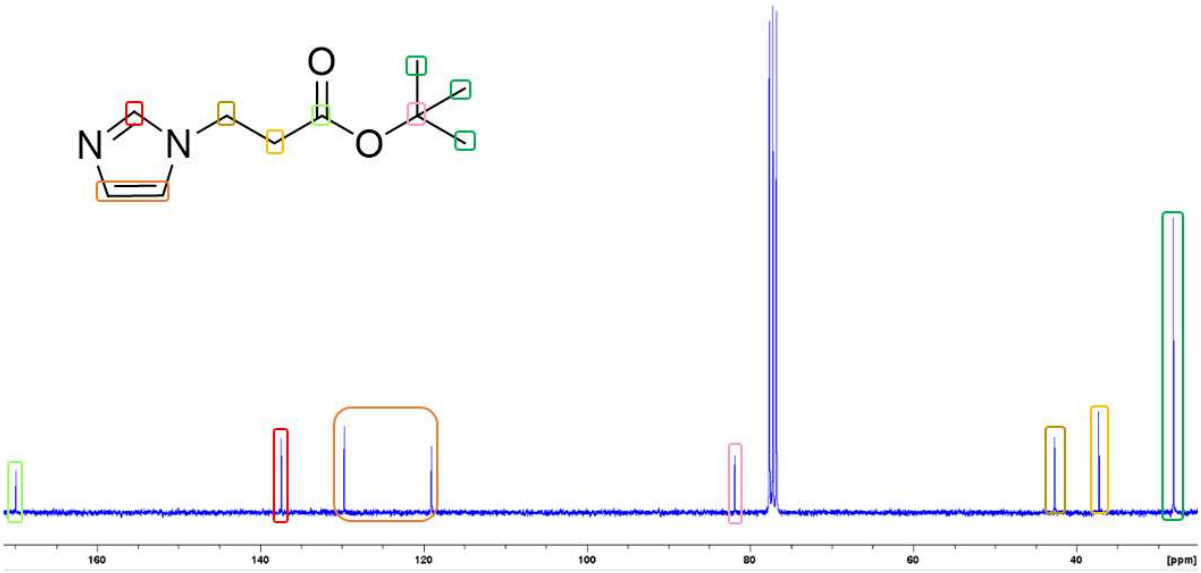

Figure 45: *^{13}C-NMR of tert-butyl 3-(1H-imidazol-1-yl)propanoate in $CDCl_3$*
M:\ICTM\ANYONE\Florian Gobec\NMR\FG31

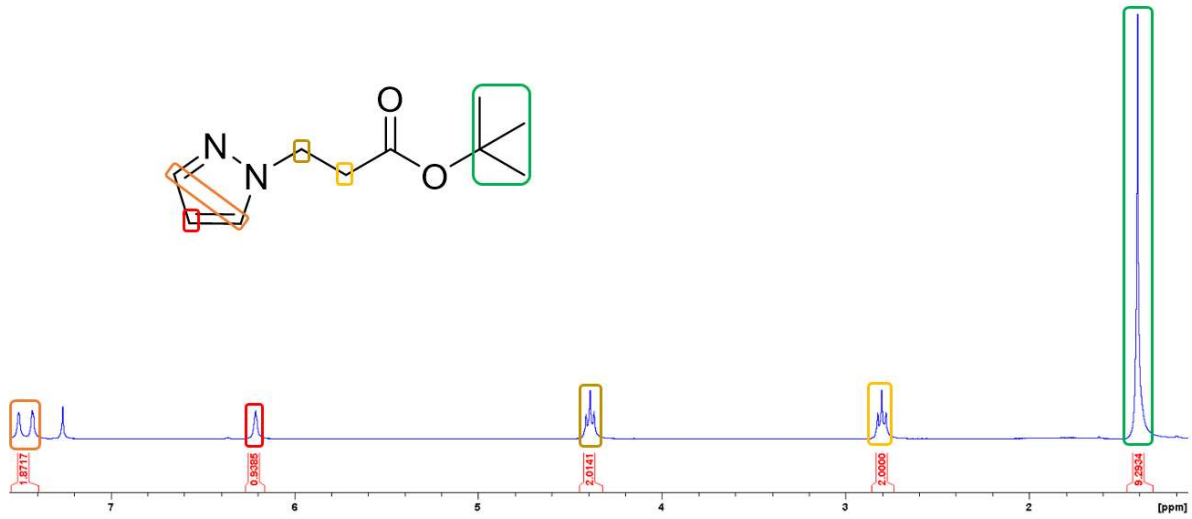

Figure 46: *^{1}H-NMR spectrum of tert-butyl 3-(1H-pyrazol-1-yl)propanoate in $CDCl_3$*
M:\ICTM\ANYONE\Florian Gobec\NMR\FG32

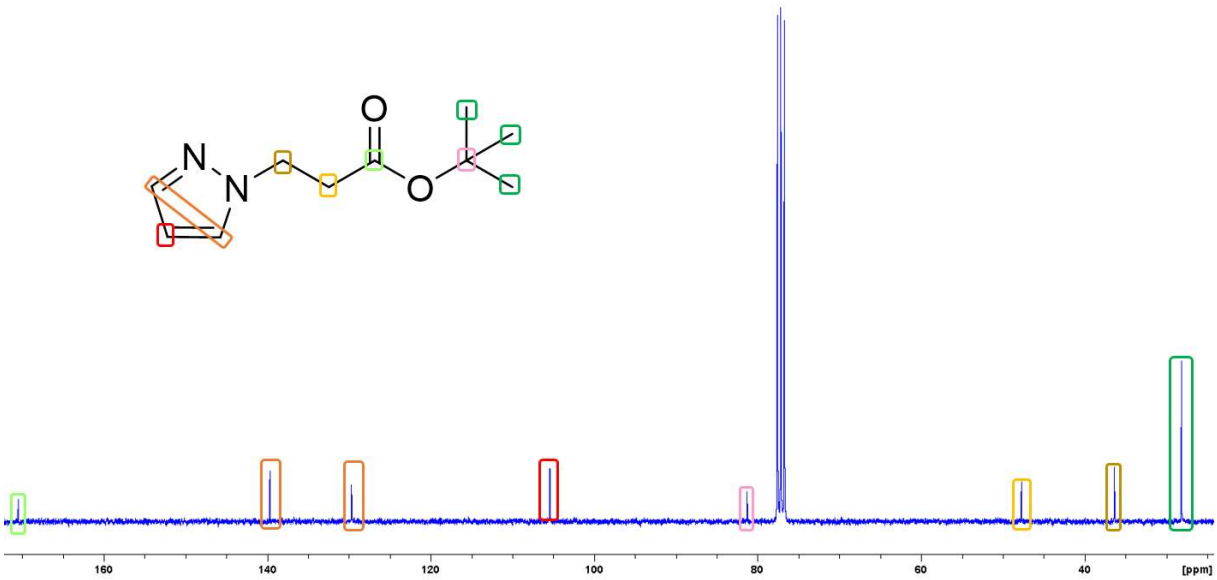

Figure 47: *^{13}C-NMR spectrum of tert-butyl 3-(1H-pyrazol-1-yl)propanoate in $CDCl_3$*
M:\ICTM\ANYONE\Florian Gobec\NMR\FG32

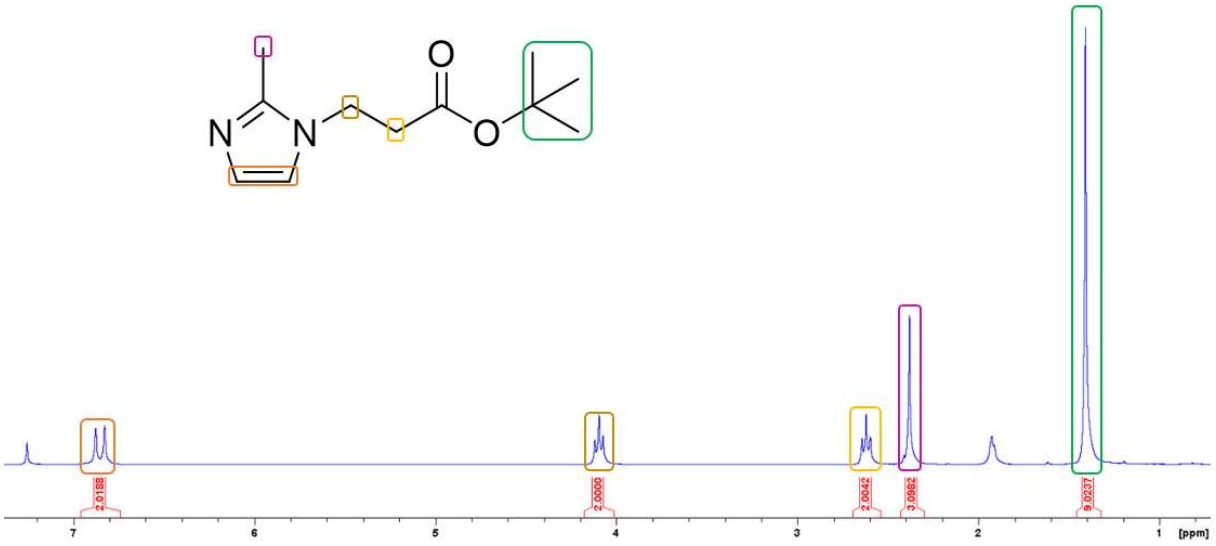

Figure 48: *^{1}H-NMR of tert-butyl 3-(2-methyl-1H-imidazol-1-yl)propanoate*
M:\ICTM\ANYONE\Florian Gobec\NMR\FG30

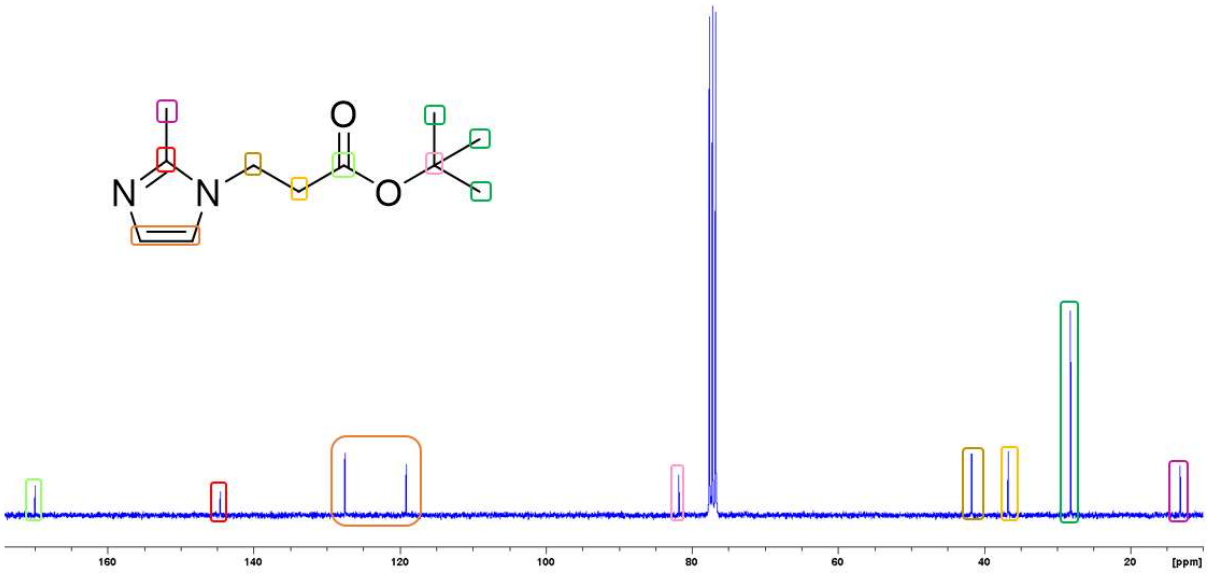

Figure 49: *^{13}C-NMR of tert-butyl 3-(2-methyl-1H-imidazol-1-yl)propanoate*
M:\ICTM\ANYONE\Florian Gobec\NMR\FG30

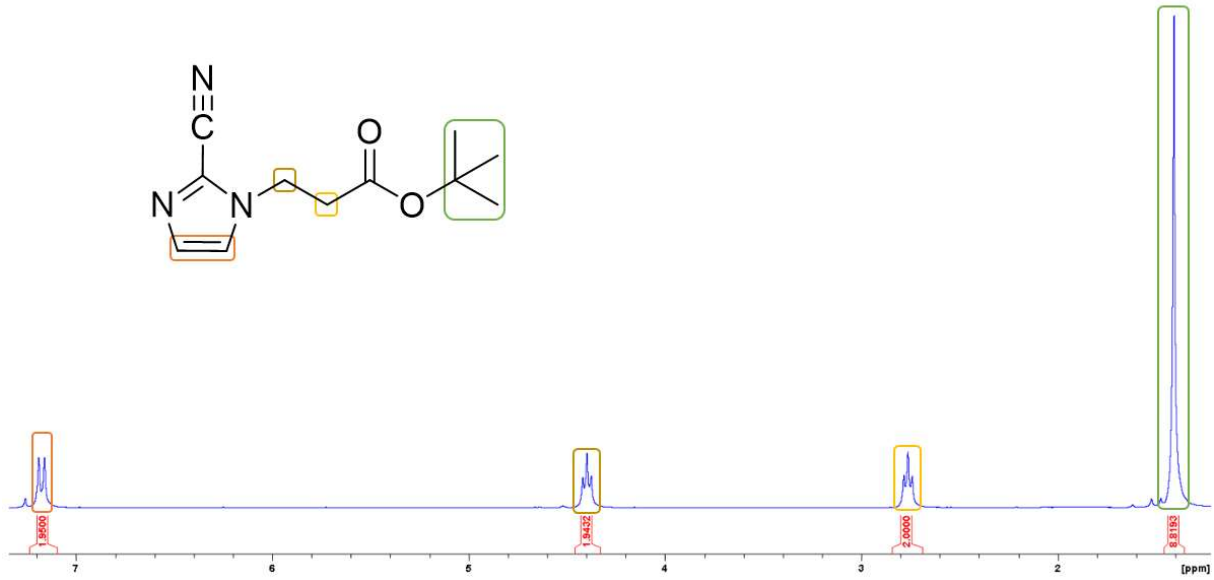

Figure 50: *^{1}H-NMR of tert-butyl 3-(2-cyano-1H-imidazol-1-yl)propanoate in $CDCl_3$*
M:\ICTM\ANYONE\Florian Gobec\NMR\FG29

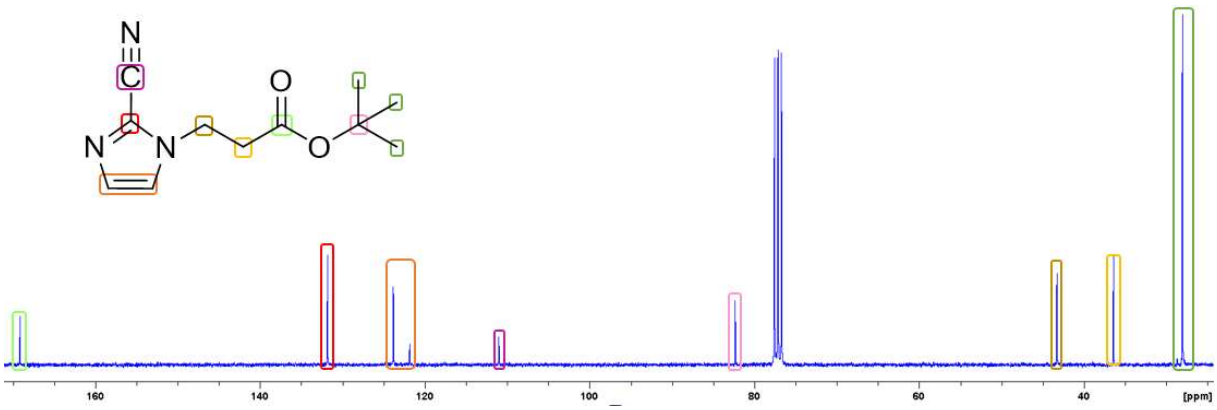

Figure 51: *^{13}C-NMR of tert-butyl 3-(2-cyano-1H-imidazol-1-yl)propanoate in $CDCl_3$*
M:\ICTM\ANYONE\Florian Gobec\NMR\FG29

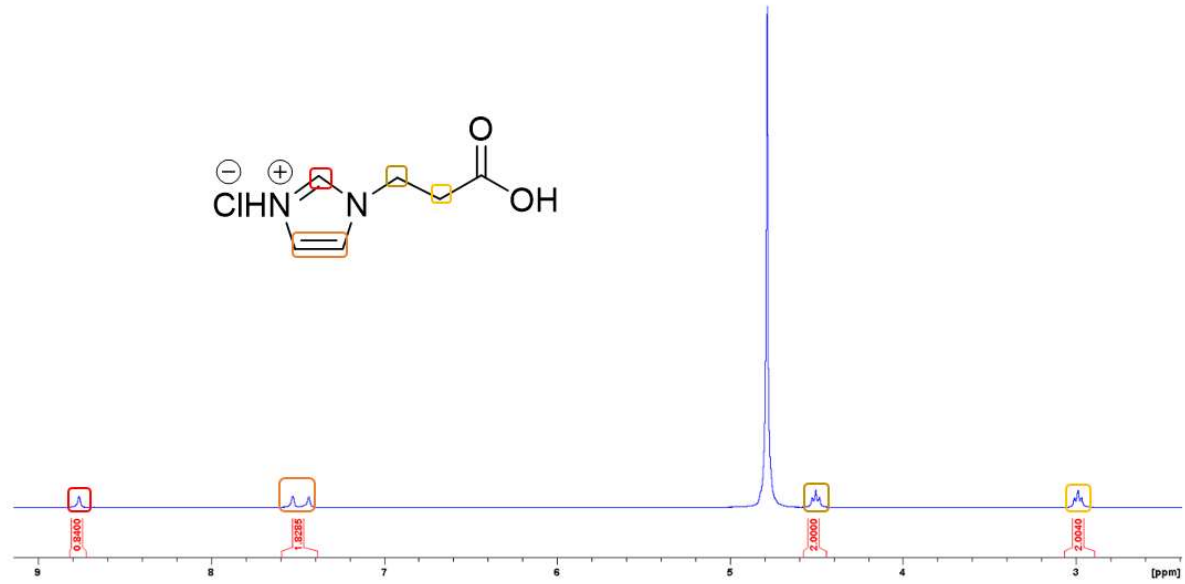

Figure 52: *^{1}H-NMR spectrum of 1-(2-carboxyethyl)-1H-imidazol-3-ium chloride in D_2O*
M:\ICTM\ANYONE\Florian Gobec\NMR\FG37

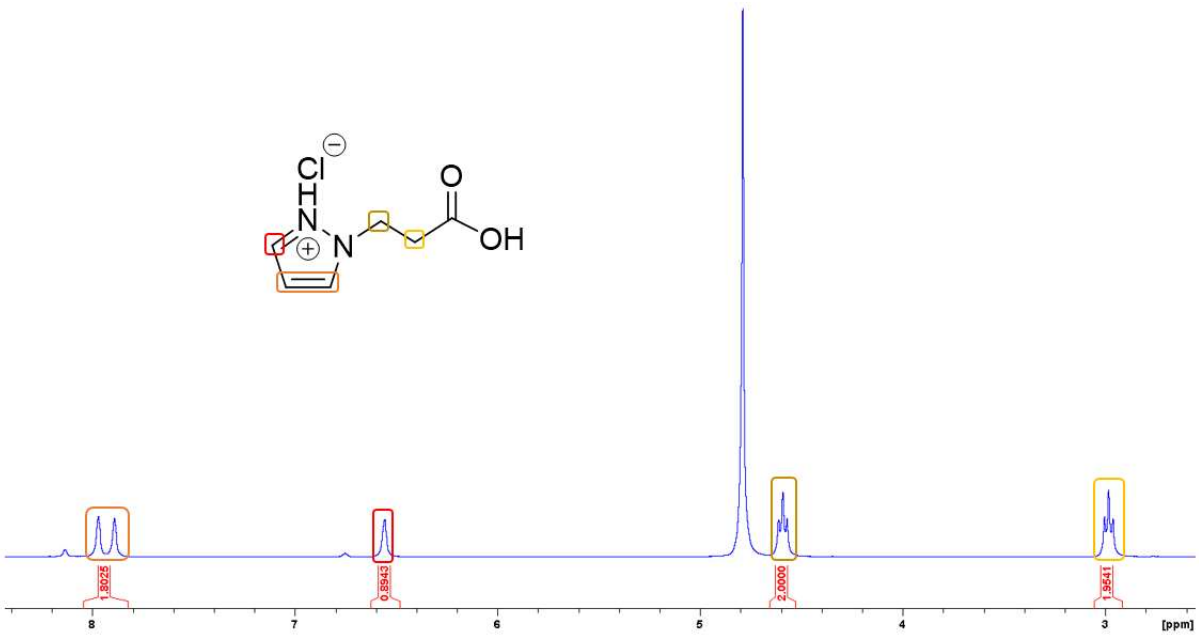

Figure 53: *^{1}H-NMR spectrum of 1-(2-carboxyethyl)-1H-pyrazol-2-ium chloride in D_2O*
M:\ICTM\ANYONE\Florian Gobec\NMR\FG39

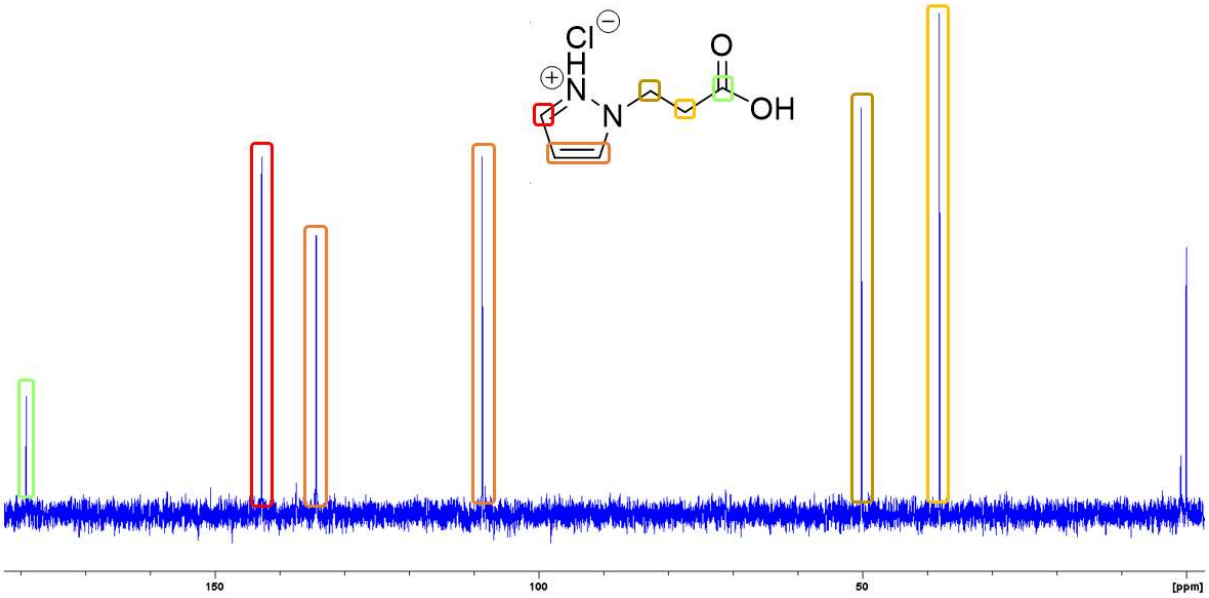

Figure 54: *^{13}C-NMR spectrum of 1-(2-carboxyethyl)-1H-pyrazol-2-ium chloride in D_2O*
M:\ICTM\ANYONE\Florian Gobec\NMR\FG39

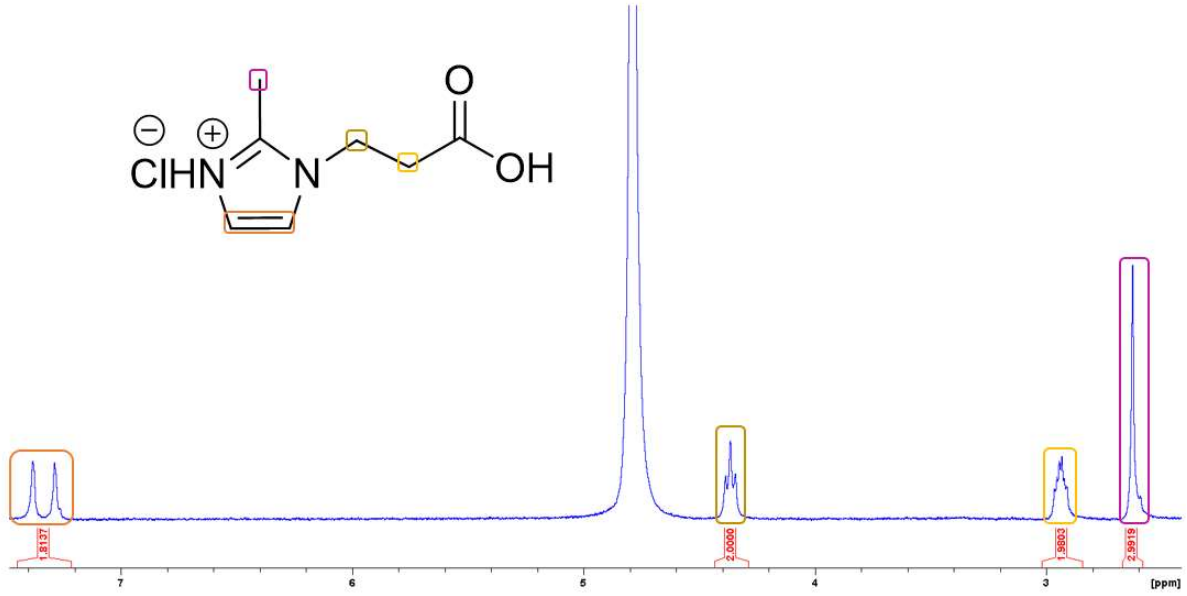

Figure 55: *^{1}H-NMR spectrum of 1-(2-carboxyethyl)-2-methyl-1H-imidazol-3-ium chloride in D_2O*
M:\ICTM\ANYONE\Florian Gobec\NMR\FG36

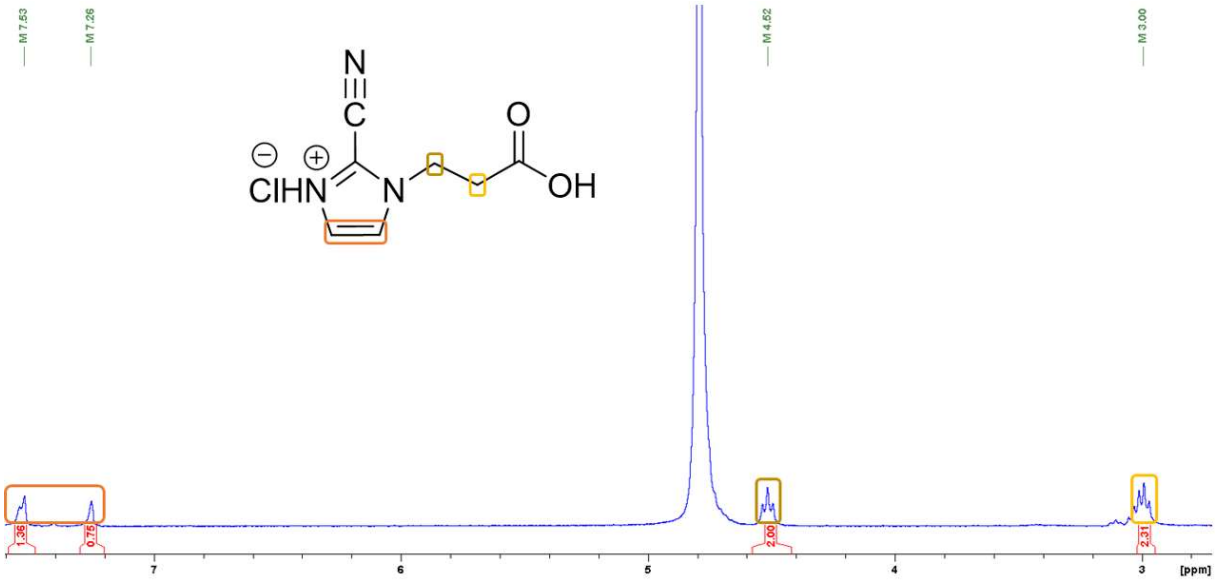

Figure 56: *^{1}H-NMR spectrum of 1-(2-carboxyethyl)-2-cyano-1H-imidazol-3-ium chloride in D_2O*
M:\ICTM\ANYONE\Florian Gobec\NMR\FG43

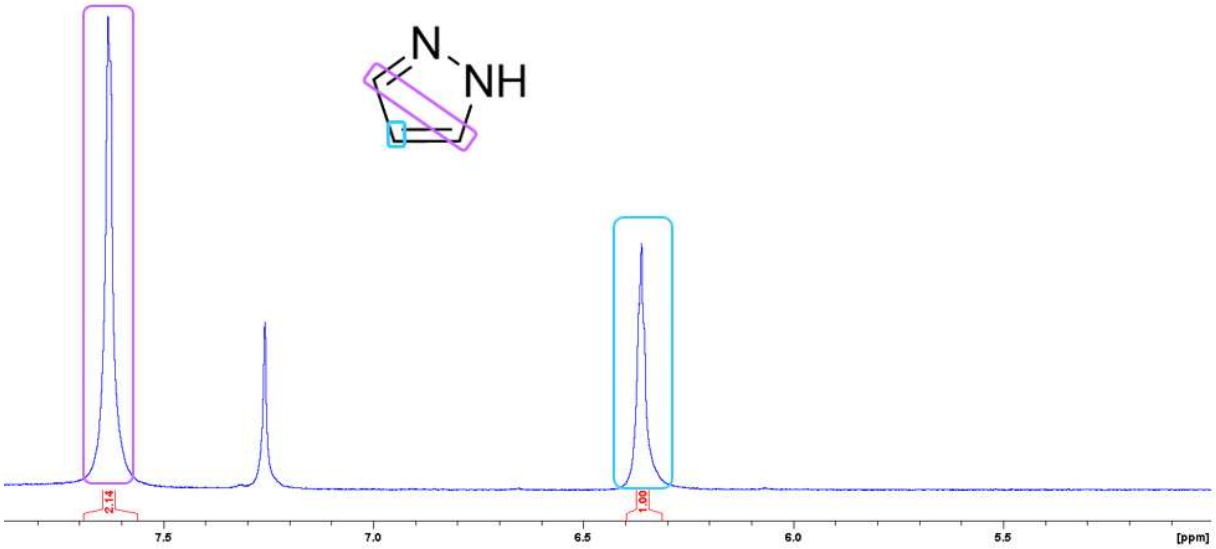

Figure 57: *^{1}H-NMR spectrum of 1H-pyrazole in $CDCl_3$*
M:\ICTM\ANYONE\Florian Gobec\NMR\Pyrazole

10.2 IR-spectra

Additional IR-spectra can be found at M:\ICTM\ANYONE\Florian Gobec\IR

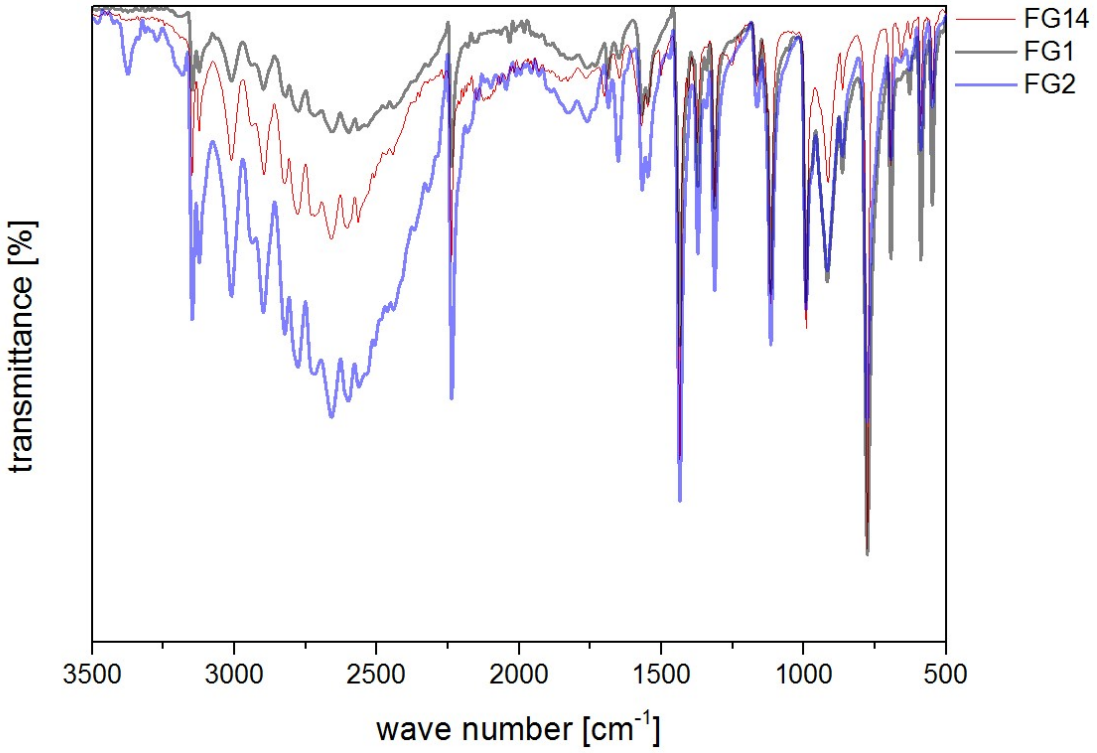

Figure 58: *IR bands of 1H-imidazole-2-carbonitrile*

M:\ICTM\ANYONE\Florian Gobec\IR\FG14

10.3 TGA-curves

The raw TGA-curves can be found at: M:\ICTM\ANYONE\Florian Gobec\TGA